Available online at www.sciencedirect.com
SCIENCE DIRECT®
International Journal of Heat and Mass Transfer 47 (2004) 613–639
International Journal of HEAT and MASS TRANSFER
www.elsevier.com/locate/ijhmt

A local thermal non-equilibrium model for two-phase flows with phase-change in porous media

F. Duval [a], F. Fichot [a,*], M. Quintard [b]

[a] Département de Recherches en Sécurité, Institut de RadioProtection et de Sûreté Nucléaire (IRSN), B.P. 3, 13115 Saint Paul Lez Durance, France

[b] Institut de Mécanique des Fluides de Toulouse (IMFT), Avenue du Professeur Camille Soula, 31400 Toulouse, France

Received 10 October 2002

Abstract

The assumption of local thermal equilibrium for describing macroscopic heat transfer in a porous medium subjected to a liquid–vapor flow with phase change has been often investigated. Under certain circumstances, this assumption appears to be too restrictive and fails to be valid. In this paper, the method of volume averaging is used to derive a three-temperature macroscopic model considering local thermal non-equilibrium between the three phases. A closed form of the evaporation rate at the macroscopic level is obtained depending on the macroscopic temperatures and the effective properties. Six pore-scale closure problems are proposed, which allow to determine all the effective transport coefficients for representative unit cells. These closure problems are solved for simple unit cells and analytical results are presented in these cases. For these simplified unit cells, a comparison between averaged temperatures obtained from direct pore-scale simulations and averaged temperatures obtained from the three-equation model has been carried out for purely diffusive phase-change processes. A good agreement is obtained between the theory and the pore-scale calculations. This confirms the validity and the practical interest of the proposed approach.

1. Introduction

Heat transfer and fluid flow with liquid–vapor phase change in porous media appears in a large number of situations of practical interest including drying processes [24], geothermal systems [71], heat-exchangers design [46], and nuclear safety analysis [45]. For the last application, there is a strong interest to understand and predict the conditions for which it is possible to cool a severely damaged reactor core.

The macroscopic description of heat transfer in a porous medium subjected to a two-phase flow with phase change is often investigated by the use of a single temperature equation. While one-equation models have been proposed recently that do not make the assumption of local equilibrium ([48], in the case of no phase change), the one-equation models are generally based on this assumption. Here, local thermal equilibrium means that the macroscopic temperatures of the three phases are close enough so that a single temperature suffices to describe the heat transport process. Although the assumption of local thermal equilibrium is acceptable in many cases of unsaturated porous media with liquid–vapor phase change, particularly for most drying processes [69], the great simplicity of the one-equation model regarding the effective transport coefficients certainly motivates its use. Nevertheless, the condition of local thermal equilibrium requires numerous constraints which have been investigated by several authors [55,58,64,68]. For instance, this condition of local equilibrium is no longer valid when the particles or pores are not small enough, when the thermal properties differ widely, or when convective transport is important. Moreover, when there is a significant heat generation in any of the phases, the system will become rapidly far from local thermal equilibrium [38]. Finally, it must be noticed too that local thermal equilibrium becomes uncertain for situations involving rapid

* Corresponding author. Fax: +33-4-42-25-64-68.
E-mail address: florian.fichot@irsn.fr (F. Fichot).

0017-9310/$ - see front matter © 2003 Elsevier Ltd. All rights reserved.
doi:10.1016/j.ijheatmasstransfer.2003.07.005

Nomenclature

$A_{\beta\gamma}$	$\beta,\gamma = g,\ell,s$, β–γ interface contained within the averaging volume, m^2
$\mathbf{b}_{\beta\gamma}$	$\beta,\gamma = g,\ell,s$, vector that maps $\langle T_\beta\rangle^\beta$ onto $\widetilde{T}_\gamma$, m
C_p	heat capacity, $J\,kg^{-1}\,K^{-1}$
ρC_p	volumetric heat capacity, $J\,m^{-3}\,K^{-1}$
$\mathbf{d}_{\gamma i}^{\beta}$	$\beta,\gamma = g,\ell,s$, non-traditional convective transport coefficient, $W\,m^{-2}\,K^{-1}$
h	enthalpy per unit mass, $J\,kg^{-1}$
h_β^{sat}	$\beta = g,\ell$, enthalpy per unit mass for the β-phase at the saturation temperature, $J\,kg^{-1}$
$\langle h_\beta\rangle^\beta$	$\beta = g,\ell,s$, intrinsic average enthalpy for the β-phase, $J\,kg^{-1}$
$\tilde{h}_\beta$	$\beta = g,\ell,s$, deviation enthalpy for the β-phase, $J\,kg^{-1}$
$h_{\gamma i}^{\beta\sigma}$	$\beta,\gamma,\sigma = g,\ell,s$ effective heat transfer coefficient, $W\,m^{-3}\,K^{-1}$
k	thermal conductivity, $W\,m^{-1}\,K^{-1}$
$\mathbf{K}_{\beta\gamma}$	$\beta,\gamma = g,\ell,s$, effective thermal dispersion tensor, $W\,m^{-1}\,K^{-1}$
l_i	$i = 1,2,3$, lattice vectors used to describe a unit cell, m
ℓ_β	$\beta = g,\ell,s$, pore-scale characteristic length for the β-phase, m
L	macroscopic characteristic length, m
$\dot{m}$	mass rate of evaporation, $kg\,m^{-3}\,s^{-1}$
$\mathbf{n}_{\beta\gamma}$	$\beta,\gamma = g,\ell,s$, unit normal vector directed from the β-phase towards the γ-phase, $\mathbf{n}_{\beta\gamma} = -\mathbf{n}_{\gamma\beta}$
r_0	radius of the averaging volume, m
$\mathbf{r}$	position vector, m
$s_{\beta i}^{\gamma}$	scalar that maps $\langle T_\beta\rangle^\beta - T^{sat}$ onto $\widetilde{T}_\gamma$
S	saturation, $S = \varepsilon_\ell/\varepsilon$
t	time, s
T_β	$\beta = g,\ell,s$, temperature in the β-phase, K
$\langle T_\beta\rangle^\beta$	$\beta = g,\ell,s$, intrinsic average temperature for the β-phase, K
$\widetilde{T}_\beta$	$\beta = g,\ell,s$, deviation temperature for the β-phase, K
T^{sat}	saturation temperature, K
$\mathbf{u}_{\beta\gamma}$	$\beta,\gamma = g,\ell,s$, non-traditional convective transport coefficient, $W\,m^{-2}\,K^{-1}$
$\mathbf{v}_\beta$	$\beta = g,\ell$, velocity in the β-phase, $m\,s^{-1}$
$\langle\mathbf{v}_\beta\rangle^\beta$	$\beta = g,\ell$, intrinsic average velocity for the β-phase, $m\,s^{-1}$
$\langle\mathbf{v}_\beta\rangle$	$\beta = g,\ell$, superficial velocity for the β-phase $\langle\mathbf{v}_\beta\rangle = \varepsilon_\beta\langle\mathbf{v}_\beta\rangle^\beta$, $m\,s^{-1}$
$\widetilde{\mathbf{v}}_\beta$	$\beta = g,\ell$, deviation velocity for the β-phase, $m\,s^{-1}$
V	averaging volume, m^3
V_β	volume of the β-phase contained within the averaging volume, m^3
$\mathbf{w}$	speed of displacement of the liquid–vapor interface, $m\,s^{-1}$

Greek symbols

Δh	heat of vaporization, $J\,kg^{-1}$
ρ	density, $kg\,m^{-3}$
η	viscosity, $N\,s\,m^{-2}$
ε_β	$\beta = g,\ell,s$, volume fraction of the β-phase
ε	porosity, $\varepsilon = 1 - \varepsilon_s$
ϖ_s	volumetric heat source, $W\,m^{-3}$

Subscripts

g	gas, vapor
ℓ	liquid
s	solid

Superscript

sat	saturation

evaporation–condensation processes. A typical example of this situation is the water flooding of an overheated porous bed in the framework of severe nuclear reactor accidents analysis. For such extreme conditions, a one-temperature description is inadequate to describe correctly both the transients associated with the quench front penetrating the hot dry porous layer and regions where dryout occurs. The first situation is analogous to the melt jets fragmentation problem where large temperature differences between phases exist and can only be dealt with by using a non-equilibrium approach [3,13]. The second situation corresponds to the prediction of critical dryout heat flux. For one-dimensional flows, the one-equation description of this problem has received considerable attention, see for instance [45,62]. For two and three-dimensional flows, the situation is quite different because hydrodynamic effects seem to play a more important role and lead to large thermal non-equilibrium which have been observed experimentally [6]. A comprehensive analysis of these non-equilibrium effects has not yet been achieved. This emphasizes the need for the development of non-equilibrium theories to describe complex two-phase flows in porous media.

When the assumption of local thermal equilibrium fails to be valid, one possible solution to model such cases is to develop separate transport equations for each phase. This leads to macroscopic models which are referred to as *non-equilibrium models*. Such models tend to become more and more popular in heat and mass transfer problems [31,50] involving large thermal or chemical constraints. For transport through a two-phase material, non-equilibrium models have been proposed

under the form of two-equation models. Such models have been studied extensively and the effective transport coefficients which appear in the macroscopic equations have been calculated for many pore-scale configurations, see for instance [53]. The validity of a two-equation description has been examined in details for the transient behavior of purely diffusive problems using a quasi-steady [58] and an unsteady two-equation model [8,47]. The first corresponds to a macroscopic model for which effective coefficients are constants while the latter corresponds to time-dependent effective coefficients which may be necessary if memory effects are important. This problem has also been addressed by comparing the quasi-steady two-equation model with a mixed formulation [32] which consists of an averaged equation for the phase with the highest conductivity coupled with a pore-scale equation for the other phase. Results of these studies indicate that the quasi-steady two-equation description is sufficient to obtain a good approximation of the problem provided thermal diffusivity ratios and temperature variation frequencies are moderate.

The problem of a two-phase flow in a porous medium with local thermal non-equilibrium has received less attention from a theoretical point of a view. A three-equation model has been developed by Petit et al. [52] using the method of volume averaging. However this model does not take into account the phase change process. On the other hand, three-equation models have been proposed heuristically such as [2,13,44,51]. As was emphasized by Quintard et al. [53], heuristic approaches lead to intuitive macroscopic models and this may lead to erroneous interpretations since these models are not derived from pore-scale transport equations through some scaling-up theory. In particular, no comprehensive approach regarding the pore-scale physics is available for the determination of the effective transport coefficients, such as the heat exchange coefficients that appear in those three-equation models. These transport coefficients could be determined experimentally but this represents a very challenging problem, especially for non-trivial situations such as those encountered in nuclear safety problems. We refer the reader to [32,34,43] for an illustration of the experimental difficulties associated with the estimate of the effective transport coefficients. Darcy's scale velocities and liquid volume fraction measurements in two-phase flows are made especially difficult and sometimes impossible in a porous medium because standard optical techniques or devices (optic fiber) cannot be used in most cases of interest (small pores, opaque particles). As a consequence, data to obtain effective properties correlations are very difficult to obtain. Owing to these experimental difficulties, effective properties of heuristic models are often extrapoled from existing correlations established in the case of single phase flow through porous media and two-phase flow in pipes. Heat exchange coefficients are also determined by using correlations based on boundary layer theory such as [9] but it has been shown [53] that such correlations do not necessarily provide good approximations. For instance, they often do not take into account the diffusive regime that occurs at low Péclet number, or they do not take into account the importance of the thermal conductivity ratio. Therefore, it appears to be important to determine the effective transport coefficients on the basis of a comprehensive analysis of the relationship between the pore-scale physics and the macroscopic description.

The purpose of this paper is to deal with the derivation of the macroscopic thermal energy transport equations in a porous medium subjected to a liquid–vapor flow with phase change using the method of volume averaging and considering local thermal non-equilibrium between the three-phases. On the basis of a steady-state closure of the problem at the microscopic scale, the method of volume averaging leads to a comprehensive generalized macroscopic three-equation model. One of the *originalities* of this study lies in the derivation of *a closed form of the mass rate of evaporation at the macroscopic level* depending on the three average temperatures and on the effective properties. Six pore-scale closure problems are provided that allow to determine all the effective transport coefficients for unit cells representative of the porous medium under consideration. In this paper, we focus our attention on simple one-dimensional unit cells for which analytical solutions can be obtained. For these simplified unit cells and for purely diffusive processes with phase change, we performed comparisons between the macro-scale model and numerical simulations at the pore-scale. For a heating problem and a temperature relaxation problem, we present comparisons between the theoretical and the numerical solutions for both the macroscopic temperatures and the liquid volume fraction evolutions.

2. Pore-scale problem

The problem under consideration corresponds to heat transfer in a three-phase system as represented in Fig. 1. We consider the flow of a liquid and its vapor in a rigid porous structure. The solid is identified as the s-phase, the liquid as the ℓ-phase, and the vapor as the g-phase. It is assumed that the physical properties of the fluids do not change strongly with temperature.

In this paper, we will adopt the drastic assumption that the two-phase flow problem can be decoupled from the heat transfer problem and can be solved independently. As a consequence, the velocity of the two phases will be assumed to be a known field. The two-phase flow macroscopic description has been extensively studied from up-scaling theories and the reader can refer to [7,41,67] for a detailed analysis of the problem. In those

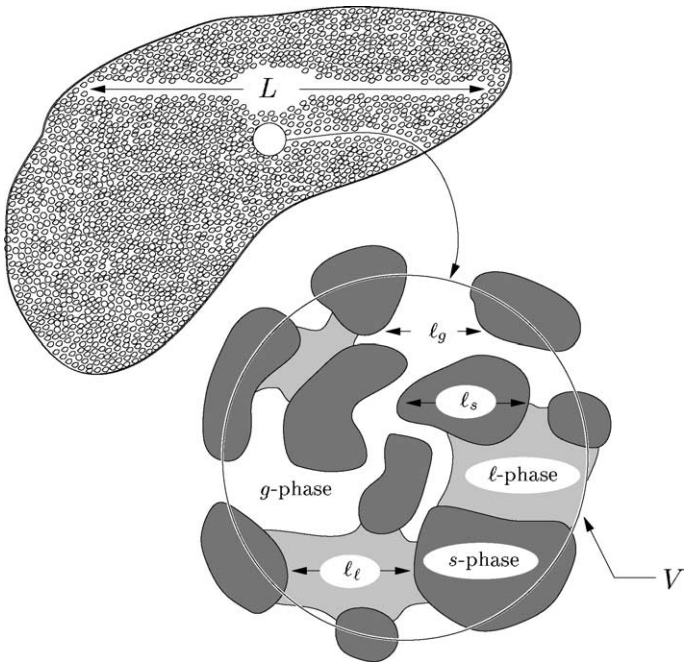

Fig. 1. Homogeneous three-phase system.

papers, a quasi-static theory has been proposed which neglects the effects associated with the possible rapid changes of the two-phase interface. In other words, if we assume that we know the position of the interface, the theory says that the form of the macro-scale equations is equivalent to extended generalized Darcy's laws. In this case, multiphase permeabilities and capillary pressure relationships can be determined from the pore-scale description. In practice, however, this is only useful if the assumptions made concerning the interface geometry are physically acceptable. Otherwise, the position of the interface must be determined by solving problems that are similar to the *original two-phase flow problem*, which is an extremely difficult task even in the case of moderately complex porous structures. We acknowledge that the above decoupling assumption may be too drastic in many situations, especially in the case of intense boiling, and this will require further analyses involving direct simulation over a significant number of pores. We believe, however, that even with this assumption, the discussion below opens interesting perspectives as far as non-equilibrium models are concerned.

We begin by the pore-scale boundary value problem that describes the mass transfer process

$$\frac{\partial \rho_{\mathrm{g}}}{\partial t} + \nabla \cdot (\rho_{\mathrm{g}} \mathbf{v}_{\mathrm{g}}) = 0, \quad \text{in the g-phase} \tag{1}$$

$$\mathbf{v}_{\mathrm{g}} = 0, \quad \text{at } A_{\mathrm{gs}} \tag{2}$$

$$\mathbf{n}_{\ell \mathrm{g}} \cdot \rho_{\mathrm{g}} (\mathbf{v}_{\mathrm{g}} - \mathbf{w}) = \mathbf{n}_{\ell \mathrm{g}} \cdot \rho_{\ell} (\mathbf{v}_{\ell} - \mathbf{w}), \quad \text{at } A_{\ell \mathrm{g}} \tag{3}$$

$$\mathbf{v}_{\ell} = 0, \quad \text{at } A_{\ell \mathrm{s}} \tag{4}$$

$$\frac{\partial \rho_{\ell}}{\partial t} + \nabla \cdot (\rho_{\ell} \mathbf{v}_{\ell}) = 0, \quad \text{in the } \ell\text{-phase} \tag{5}$$

Here $\mathbf{w}$ is the liquid–vapor interface velocity, $\mathbf{n}_{\ell \mathrm{g}}$ represents the unit normal directed from the ℓ-phase towards the g-phase and $A_{\ell \mathrm{g}}$ is the ℓ–g interface. On the other hand, the pore-scale heat transfer problem in the three-phase system is described in terms of the following governing differential equations

$$\frac{\partial \rho_{\mathrm{g}} h_{\mathrm{g}}}{\partial t} + \nabla \cdot (\rho_{\mathrm{g}} h_{\mathrm{g}} \mathbf{v}_{\mathrm{g}}) = \nabla \cdot (k_{\mathrm{g}} \nabla T_{\mathrm{g}}), \quad \text{in the g-phase} \tag{6}$$

$$\frac{\partial \rho_{\ell} h_{\ell}}{\partial t} + \nabla \cdot (\rho_{\ell} h_{\ell} \mathbf{v}_{\ell}) = \nabla \cdot (k_{\ell} \nabla T_{\ell}), \quad \text{in the } \ell\text{-phase} \tag{7}$$

$$\frac{\partial \rho_{\mathrm{s}} h_{\mathrm{s}}}{\partial t} = \nabla \cdot (k_{\mathrm{s}} \nabla T_{\mathrm{s}}) + \varpi_{\mathrm{s}}, \quad \text{in the s-phase} \tag{8}$$

where ϖ_{s} represents a constant homogeneous volumetric thermal source in the solid phase. Here we have neglected compression work, viscous dissipation and radiation exchange. The boundary conditions at the liquid–solid and vapor–solid interfaces express continuity of both temperatures and heat fluxes

$$T_{\mathrm{g}} = T_{\mathrm{s}}, \quad \mathbf{n}_{\mathrm{gs}} \cdot k_{\mathrm{g}} \nabla T_{\mathrm{g}} = \mathbf{n}_{\mathrm{gs}} \cdot k_{\mathrm{s}} \nabla T_{\mathrm{s}} \quad \text{at } A_{\mathrm{gs}} \tag{9}$$

$$T_{\ell} = T_{\mathrm{s}}, \quad \mathbf{n}_{\ell \mathrm{s}} \cdot k_{\ell} \nabla T_{\ell} = \mathbf{n}_{\ell \mathrm{s}} \cdot k_{\mathrm{s}} \nabla T_{\mathrm{s}} \quad \text{at } A_{\ell \mathrm{s}} \tag{10}$$

The boundary conditions at the liquid–vapor interface are more complex because phase change takes place at

this interface. It is quite reasonable to assume that the vapor phase is in thermodynamical equilibrium with the liquid phase at the ℓ–g interface. This basically means that the interface temperature is fixed at the equilibrium saturation temperature T^{sat}. Under these circumstances, the boundary conditions at the liquid–vapor interface are written as

$$T_\ell = T_{\mathrm{g}} = T^{\mathrm{sat}} \quad \text{at } A_{\ell\mathrm{g}} \tag{11}$$

$$\mathbf{n}_{\ell\mathrm{g}} \cdot (-k_{\mathrm{g}} \nabla T_{\mathrm{g}} + \rho_{\mathrm{g}} h_{\mathrm{g}} (\mathbf{v}_{\mathrm{g}} - \mathbf{w})) = \mathbf{n}_{\ell\mathrm{g}} \cdot (-k_\ell \nabla T_\ell + \rho_\ell h_\ell (\mathbf{v}_\ell - \mathbf{w})) \quad \text{at } A_{\ell\mathrm{g}} \tag{12}$$

As pointed out by Quintard and Whitaker [57] in an analog case for mass transfer processes, the condition (11) is referred to as *local thermodynamic equilibrium* and does not have to be confused with the assumption of *local thermal equilibrium*. In addition to Eqs. (10)–(12), boundary conditions at the entrances and the exits of the medium and initial conditions must be prescribed in order to solve the problem and we refer to [70] for their treatment.

3. Volume averaging

In this paper, our objective is to develop a three-temperature macroscopic model using the method of volume averaging. In this method, an averaging volume V is associated with every point in space as illustrated in Fig. 1. Then, the macroscopic transport equations can be obtained by averaging the pore-scale transport equations over this volume. The length scale constraints required in the method of volume averaging are discussed in details elsewhere [18,55] and here we note only that the averaging volume must be large compared with the pore-scale characteristic lengths ℓ_{g}, ℓ_ℓ and ℓ_{s} but small compared to the macroscopic characteristic length L. For some function ψ_β associated with the β-phase, we define two different averages, the phase average $\langle \psi_\beta \rangle$ and the intrinsic phase average $\langle \psi_\beta \rangle^\beta$. These two averages are defined according to

$$\langle \psi_\beta \rangle = \frac{1}{V} \int_{V_\beta} \psi_\beta \, \mathrm{d}V, \quad \langle \psi_\beta \rangle^\beta = \frac{1}{V_\beta} \int_{V_\beta} \psi_\beta \, \mathrm{d}V, \quad \langle \psi_\beta \rangle = \varepsilon_\beta \langle \psi_\beta \rangle^\beta \tag{13}$$

in which V_β represents the volume of the β-phase contained within the averaging volume and ε_β is the volume fraction of the β-phase ($\varepsilon_{\mathrm{g}} + \varepsilon_\ell + \varepsilon_{\mathrm{s}} = 1$). The point values ψ_β in the β-phase are related to the intrinsic phase average $\langle \psi_\beta \rangle^\beta$ and the pore-scale deviation $\tilde{\psi}_\beta$ according to Gray's [33] spatial decomposition

$$\psi_\beta = \langle \psi_\beta \rangle^\beta + \tilde{\psi}_\beta \tag{14}$$

3.1. Mass transport

Before dealing with the averaging process associated with the heat transport problem, we first recall the volume averaged forms of the continuity equations. We simply list below the major steps leading to the macroscopic forms, more details can be found in [69]. The volume averaging of the pore-scale mass transport equations (1) and (5) leads to

$$\frac{\partial \varepsilon_{\mathrm{g}} \langle \rho_{\mathrm{g}} \rangle^{\mathrm{g}}}{\partial t} + \nabla \cdot \langle \rho_{\mathrm{g}} \mathbf{v}_{\mathrm{g}} \rangle = -\frac{1}{V} \int_{A_{\mathrm{g}\ell}} \mathbf{n}_{\mathrm{g}\ell} \cdot \rho_{\mathrm{g}} (\mathbf{v}_{\mathrm{g}} - \mathbf{w}) \, \mathrm{d}A \tag{15}$$

$$\frac{\partial \varepsilon_\ell \rho_\ell}{\partial t} + \nabla \cdot (\rho_\ell \langle \mathbf{v}_\ell \rangle) = -\frac{1}{V} \int_{A_{\ell\mathrm{g}}} \mathbf{n}_{\ell\mathrm{g}} \cdot \rho_\ell (\mathbf{v}_\ell - \mathbf{w}) \, \mathrm{d}A \tag{16}$$

where we have made use of the general transport theorem and the spatial averaging theorem [66]. We define the mass rate of evaporation $\dot{m}$ according to

$$\dot{m} = -\frac{1}{V} \int_{A_{\mathrm{g}\ell}} \mathbf{n}_{\mathrm{g}\ell} \cdot \rho_{\mathrm{g}} (\mathbf{v}_{\mathrm{g}} - \mathbf{w}) \, \mathrm{d}A \tag{17}$$

Because of the boundary condition Eq. (3), this definition leads to the following continuity macroscopic equations

$$\frac{\partial \varepsilon_{\mathrm{g}} \rho_{\mathrm{g}}}{\partial t} + \nabla \cdot (\rho_{\mathrm{g}} \langle \mathbf{v}_{\mathrm{g}} \rangle) = \dot{m} \tag{18}$$

$$\frac{\partial \varepsilon_\ell \rho_\ell}{\partial t} + \nabla \cdot (\rho_\ell \langle \mathbf{v}_\ell \rangle) = -\dot{m} \tag{19}$$

where $\langle \mathbf{v}_{\mathrm{g}} \rangle$ and $\langle \mathbf{v}_\ell \rangle$ are the superficial or Darcy's velocities. In these equations, it has been assumed that both the liquid and vapor phase densities do not vary significantly *within the averaging volume*. As a consequence, the point densities ρ_{g} and ρ_ℓ can be identified with the intrinsic phase average densities $\langle \rho_{\mathrm{g}} \rangle^{\mathrm{g}}$ and $\langle \rho_\ell \rangle^\ell$. However, it must be noted that neglecting variations within the averaging volume does not mean that the densities will be constants at the macroscopic scale [69]. To be explicit about this point, $\langle \rho_{\mathrm{g}} \rangle^{\mathrm{g}}$ is replaced in the macroscale equations by

$$\langle \rho_{\mathrm{g}} \rangle^{\mathrm{g}} = \rho_{\mathrm{g}} (\langle p_{\mathrm{g}} \rangle^{\mathrm{g}}, \langle T_{\mathrm{g}} \rangle^{\mathrm{g}}) \tag{20}$$

3.2. Energy transport

We are now ready to form the phase average of Eqs. (6)–(8). Starting with the pore-scale thermal energy equation for the g-phase, we form the phase average to obtain

$$\left\langle \frac{\partial \rho_{\mathrm{g}} h_{\mathrm{g}}}{\partial t} \right\rangle + \langle \nabla \cdot (\rho_{\mathrm{g}} h_{\mathrm{g}} \mathbf{v}_{\mathrm{g}}) \rangle = \langle \nabla \cdot (k_{\mathrm{g}} \nabla T_{\mathrm{g}}) \rangle \tag{21}$$

Once again we ignore variations of the physical properties within the averaging volume. The application of

the general transport theorem and the spatial averaging theorem leads to

$$\frac{\partial \rho_g \langle h_g \rangle}{\partial t} + \nabla \cdot \langle \rho_g h_g \mathbf{v}_g \rangle + \frac{1}{V}\int_{A_{g\ell}} \mathbf{n}_{g\ell} \cdot \rho_g h_g (\mathbf{v}_g - \mathbf{w})\, dA = \nabla \cdot \langle k_g \nabla T_g \rangle + \frac{1}{V}\int_{A_{g\ell}} \mathbf{n}_{g\ell} \cdot k_g \nabla T_g\, dA + \frac{1}{V}\int_{A_{gs}} \mathbf{n}_{gs} \cdot k_g \nabla T_g\, dA \quad (22)$$

One can follow previous studies [18,33,61,73] in order to express Eq. (22) as

$$\frac{\partial \varepsilon_g \rho_g \langle h_g \rangle^g}{\partial t} + \nabla \cdot (\varepsilon_g \rho_g \langle h_g \rangle^g \langle \mathbf{v}_g \rangle^g) + \nabla \cdot \langle \rho_g \tilde{h}_g \tilde{\mathbf{v}}_g \rangle + \frac{1}{V}\int_{A_{g\ell}} \mathbf{n}_{g\ell} \cdot \rho_g h_g (\mathbf{v}_g - \mathbf{w})\, dA = \nabla \cdot \left(\varepsilon_g k_g \nabla \langle T_g \rangle^g + \frac{1}{V}\int_{A_{g\ell}} \mathbf{n}_{g\ell} k_g \widetilde{T}_g\, dA + \frac{1}{V}\int_{A_{gs}} \mathbf{n}_{gs} k_g \widetilde{T}_g\, dA \right) - \nabla \varepsilon_g \cdot k_g \nabla \langle T_g \rangle^g + \frac{1}{V}\int_{A_{g\ell}} \mathbf{n}_{g\ell} \cdot k_g \nabla \widetilde{T}_g\, dA + \frac{1}{V}\int_{A_{gs}} \mathbf{n}_{gs} \cdot k_g \nabla \widetilde{T}_g\, dA \quad (23)$$

Here we have used the following spatial decompositions

$$h_g = \langle h_g \rangle^g + \tilde{h}_g, \quad T_g = \langle T_g \rangle^g + \widetilde{T}_g, \quad \mathbf{v}_g = \langle \mathbf{v}_g \rangle^g + \tilde{\mathbf{v}}_g \quad (24)$$

It is beyond the scope of this paper to recall the developments leading to Eq. (23) and we refer the reader to the literature cited above for a complete analysis. Using the macroscopic mass transport equation for the g-phase equation (18), one can obtain a more convenient form of the left hand side of Eq. (23) given by

$$\varepsilon_g \rho_g \frac{\partial \langle h_g \rangle^g}{\partial t} + \rho_g \langle \mathbf{v}_g \rangle \cdot \nabla \langle h_g \rangle^g + \nabla \cdot \langle \rho_g \tilde{h}_g \tilde{\mathbf{v}}_g \rangle + \frac{1}{V}\int_{A_{g\ell}} \mathbf{n}_{g\ell} \cdot \rho_g (h_g - \langle h_g \rangle^g)(\mathbf{v}_g - \mathbf{w})\, dA \quad (25)$$

At this point, we express the point enthalpy–temperature relationship as

$$h_g = h_g^{sat} + C_{pg}(T_g - T^{sat}) \quad (26)$$

$$h_\ell = h_\ell^{sat} + C_{p\ell}(T_\ell - T^{sat}) \quad (27)$$

$$h_s = C_{ps} T_s + h_s^0 \quad (28)$$

Ignoring variations of the physical properties *within the averaging volume*, these relations lead to the following relations for the g-phase intrinsic average and the g-phase spatial deviation

$$\langle h_g \rangle^g = h_g^{sat} + C_{pg}(\langle T_g \rangle^g - T^{sat}) \quad (29)$$

$$\tilde{h}_g = C_{pg} \widetilde{T}_g \quad (30)$$

We refer here to [36] for a more detailed treatment of the constraints leading to such an average enthalpy–temperature relationship. From Eqs. (29) and (30), expression (25) takes the form

$$\varepsilon_g (\rho C_p)_g \left(\frac{\partial \langle T_g \rangle^g}{\partial t} + \langle \mathbf{v}_g \rangle^g \cdot \nabla \langle T_g \rangle^g \right) + \nabla \cdot ((\rho C_p)_g \langle \widetilde{T}_g \tilde{\mathbf{v}}_g \rangle) + \frac{1}{V}\int_{A_{g\ell}} \mathbf{n}_{g\ell} \cdot (\rho C_p)_g \widetilde{T}_g (\mathbf{v}_g - \mathbf{w})\, dA \quad (31)$$

The last term of Eq. (31) represents a phase change term and it can be written explicitly in term of the mass rate of evaporation $\dot{m}$. To do so, we first remark that the g-phase temperature can be decomposed according to Eq. (24) and one can use this decomposition in order to express the thermodynamic equilibrium boundary condition (11) as

$$\widetilde{T}_g = T^{sat} - \langle T_g \rangle^g, \quad \text{on } A_{\ell g} \quad (32)$$

When both $\langle T_g \rangle^g$ and the saturation temperature are removed from the integral of expression (31), we can use the mass rate of evaporation definition Eq. (17) to express the phase change term as

$$\frac{1}{V}\int_{A_{g\ell}} \mathbf{n}_{g\ell} \cdot (\rho C_p)_g \widetilde{T}_\ell (\mathbf{v}_g - \mathbf{w})\, dA = -\dot{m} C_{pg} (T^{sat} - \langle T_g \rangle^g) \quad (33)$$

where we have again ignored variations of the physical properties within the averaging volume. We can now use Eq. (33) with expression (31) in the left hand side of Eq. (23) to obtain the following form of the volume averaged energy transport equation for the g-phase

$$\varepsilon_g (\rho C_p)_g \left(\frac{\partial \langle T_g \rangle^g}{\partial t} + \langle \mathbf{v}_g \rangle^g \cdot \nabla \langle T_g \rangle^g \right) + \nabla \cdot ((\rho C_p)_g \langle \widetilde{T}_g \tilde{\mathbf{v}}_g \rangle) - \dot{m} C_{pg} (T^{sat} - \langle T_g \rangle^g) = \nabla \cdot \left(\varepsilon_g k_g \nabla \langle T_g \rangle^g + \frac{1}{V}\int_{A_{g\ell}} \mathbf{n}_{g\ell} k_g \widetilde{T}_g\, dA + \frac{1}{V}\int_{A_{gs}} \mathbf{n}_{gs} k_g \widetilde{T}_g\, dA \right) - \nabla \varepsilon_g \cdot k_g \nabla \langle T_g \rangle^g + \frac{1}{V}\int_{A_{g\ell}} \mathbf{n}_{g\ell} \cdot k_g \nabla \widetilde{T}_g\, dA + \frac{1}{V}\int_{A_{gs}} \mathbf{n}_{gs} \cdot k_g \nabla \widetilde{T}_g\, dA \quad (34)$$

Equations similar to Eq. (34) are available for the ℓ-phase and the s-phase, and they are written below without further development

$$\varepsilon_\ell(\rho C_p)_\ell\left(\frac{\partial\langle T_\ell\rangle^\ell}{\partial t}+\langle\mathbf{v}_\ell\rangle^\ell\cdot\nabla\langle T_\ell\rangle^\ell\right)+\nabla\cdot\left((\rho C_p)_\ell\langle\widetilde{T}_\ell\tilde{\mathbf{v}}_\ell\rangle\right)+\dot{m}C_{p\ell}(T^{\mathrm{sat}}-\langle T_\ell\rangle^\ell)$$
$$=\nabla\cdot\left(\varepsilon_\ell k_\ell\nabla\langle T_\ell\rangle^\ell+\frac{1}{V}\int_{A_{\ell\mathrm{g}}}\mathbf{n}_{\ell\mathrm{g}}k_\ell\widetilde{T}_\ell\,\mathrm{d}A+\frac{1}{V}\int_{A_{\ell\mathrm{s}}}\mathbf{n}_{\ell\mathrm{s}}k_\ell\widetilde{T}_\ell\,\mathrm{d}A\right)-\nabla\varepsilon_\ell\cdot k_\ell\nabla\langle T_\ell\rangle^\ell+\frac{1}{V}\int_{A_{\ell\mathrm{g}}}\mathbf{n}_{\ell\mathrm{g}}\cdot k_\ell\nabla\widetilde{T}_\ell\,\mathrm{d}A+\frac{1}{V}\int_{A_{\ell\mathrm{s}}}\mathbf{n}_{\ell\mathrm{s}}\cdot k_\ell\nabla\widetilde{T}_\ell\,\mathrm{d}A \quad (35)$$

$$\varepsilon_{\mathrm{s}}(\rho C_p)_{\mathrm{s}}\frac{\partial\langle T_{\mathrm{s}}\rangle^{\mathrm{s}}}{\partial t}=\nabla\cdot\left(\varepsilon_{\mathrm{s}}k_{\mathrm{s}}\nabla\langle T_{\mathrm{s}}\rangle^{\mathrm{s}}+\frac{1}{V}\int_{A_{\mathrm{s}\ell}}\mathbf{n}_{\mathrm{s}\ell}k_{\mathrm{s}}\widetilde{T}_{\mathrm{s}}\,\mathrm{d}A+\frac{1}{V}\int_{A_{\mathrm{sg}}}\mathbf{n}_{\mathrm{sg}}k_{\mathrm{s}}\widetilde{T}_{\mathrm{s}}\,\mathrm{d}A\right)-\nabla\varepsilon_{\mathrm{s}}\cdot k_{\mathrm{s}}\nabla\langle T_{\mathrm{s}}\rangle^{\mathrm{s}}+\frac{1}{V}\int_{A_{\mathrm{s}\ell}}\mathbf{n}_{\mathrm{s}\ell}\cdot k_{\mathrm{s}}\nabla\widetilde{T}_{\mathrm{s}}\,\mathrm{d}A+\frac{1}{V}\int_{A_{\mathrm{sg}}}\mathbf{n}_{\mathrm{sg}}\cdot k_{\mathrm{s}}\nabla\widetilde{T}_{\mathrm{s}}\,\mathrm{d}A+\varepsilon_{\mathrm{s}}\langle\varpi_{\mathrm{s}}\rangle^{\mathrm{s}} \quad (36)$$

4. Closure

Since the temperature deviations appear in the averaged transport equations (34)–(36), one needs to develop boundary value problems for these deviations. To obtain a governing equation for the deviation $\widetilde{T}_{\mathrm{g}}$, we return to the pore-scale transport equation (6), introduce Gray's decomposition equation (14), and subtract the result from Eq. (34) divided by ε_{g}. The resulting pore-scale equation for $\widetilde{T}_{\mathrm{g}}$ is written as

$$(\rho C_p)_{\mathrm{g}}\frac{\partial\widetilde{T}_{\mathrm{g}}}{\partial t}+(\rho C_p)_{\mathrm{g}}\mathbf{v}_{\mathrm{g}}\cdot\nabla\widetilde{T}_{\mathrm{g}}+(\rho C_p)_{\mathrm{g}}\tilde{\mathbf{v}}_{\mathrm{g}}\cdot\nabla\langle T_{\mathrm{g}}\rangle^{\mathrm{g}}-\varepsilon_{\mathrm{g}}^{-1}\nabla\cdot\left((\rho C_p)_{\mathrm{g}}\langle\widetilde{T}_{\mathrm{g}}\tilde{\mathbf{v}}_{\mathrm{g}}\rangle\right)+\varepsilon_{\mathrm{g}}^{-1}\dot{m}C_{p\mathrm{g}}(T^{\mathrm{sat}}-\langle T_{\mathrm{g}}\rangle^{\mathrm{g}})$$
$$=\nabla\cdot(k_{\mathrm{g}}\nabla\widetilde{T}_{\mathrm{g}})-\varepsilon_{\mathrm{g}}^{-1}\nabla\cdot\left(\frac{1}{V}\int_{A_{\mathrm{g}\ell}}\mathbf{n}_{\mathrm{g}\ell}k_{\mathrm{g}}\widetilde{T}_{\mathrm{g}}\,\mathrm{d}A+\frac{1}{V}\int_{A_{\mathrm{gs}}}\mathbf{n}_{\mathrm{gs}}k_{\mathrm{g}}\widetilde{T}_{\mathrm{g}}\,\mathrm{d}A\right)-\varepsilon_{\mathrm{g}}^{-1}\left(\frac{1}{V}\int_{A_{\mathrm{g}\ell}}\mathbf{n}_{\mathrm{g}\ell}\cdot k_{\mathrm{g}}\nabla\widetilde{T}_{\mathrm{g}}\,\mathrm{d}A+\frac{1}{V}\int_{A_{\mathrm{gs}}}\mathbf{n}_{\mathrm{gs}}\cdot k_{\mathrm{g}}\nabla\widetilde{T}_{\mathrm{g}}\,\mathrm{d}A\right) \quad (37)$$

This result can be simplified by estimating the order of magnitude of its different terms. This has been done for instance by Carbonell and Whitaker [18] and Quintard and Whitaker [55,61]. According to these previous developments, on the basis of the length-scale constraint $\ell_{\mathrm{g}}\ll L$, we can simplify Eq. (37) to obtain

$$(\rho C_p)_{\mathrm{g}}\frac{\partial\widetilde{T}_{\mathrm{g}}}{\partial t}+(\rho C_p)_{\mathrm{g}}\mathbf{v}_{\mathrm{g}}\cdot\nabla\widetilde{T}_{\mathrm{g}}+(\rho C_p)_{\mathrm{g}}\tilde{\mathbf{v}}_{\mathrm{g}}\cdot\nabla\langle T_{\mathrm{g}}\rangle^{\mathrm{g}}+\varepsilon_{\mathrm{g}}^{-1}\dot{m}C_{p\mathrm{g}}(T^{\mathrm{sat}}-\langle T_{\mathrm{g}}\rangle^{\mathrm{g}})$$
$$=\nabla\cdot(k_{\mathrm{g}}\nabla\widetilde{T}_{\mathrm{g}})-\varepsilon_{\mathrm{g}}^{-1}\left(\frac{1}{V}\int_{A_{\mathrm{g}\ell}}\mathbf{n}_{\mathrm{g}\ell}\cdot k_{\mathrm{g}}\nabla\widetilde{T}_{\mathrm{g}}\,\mathrm{d}A+\frac{1}{V}\int_{A_{\mathrm{gs}}}\mathbf{n}_{\mathrm{gs}}\cdot k_{\mathrm{g}}\nabla\widetilde{T}_{\mathrm{g}}\,\mathrm{d}A\right) \quad (38)$$

Similar governing equations can be obtained for $\widetilde{T}_\ell$ and $\widetilde{T}_{\mathrm{s}}$ following the same procedure. Boundary conditions for the spatial deviations can be derived from boundary conditions (9)–(11) using spatial decompositions such as the one given by Eq. (14).

At this point, to obtain a macroscopic description of the three-phase system, we need to solve simultaneously the macroscopic transport equations (34)–(36), together with the pore-scale boundary value problem for the deviations $\widetilde{T}_{\mathrm{g}}$, $\widetilde{T}_\ell$ and $\widetilde{T}_{\mathrm{s}}$. This leads to a *more complex problem* and thus motivates us to make some simplifications and to construct an *approximate solution*.

All these simplifications will be discussed on the basis of the more exhaustively studied two-phase system case. First we will dismiss the case of local thermal equilibrium for which a single temperature treatment can be used, and we refer the reader to the literature on the subject for an approximate solution of the coupled micro-scale and averaged equations (see for instance [37,56,70] for an approach using the theory of volume averaging or [15,16,29] for a treatment using the homogenization theory). Non-equilibrium situations in the case of purely diffusive systems has received a lot of attention. In this discussion, we will make use of the literature about thermal diffusion, but also on works based on the equations describing the flow of a slightly compressible fluid [21], which have the same mathematical structure. The elements of the discussion are summarized below.

Given the nature of the coupled equations, there is a strong potential for the solution showing non-local behavior in space and time [12,23,39], i.e., the solution of the coupled equations features historical behavior involving the history at all points within the domain. All the literature is about approximate solutions to avoid such a complicated treatment. The first approximation historically used led to a fully macro-scale model involving two macro-scale equations [10,18,55,58,73]. This development implies a quasi-steady treatment of the deviation equations, i.e., the time derivative is formally suppressed in these equations. The temperature deviations are expressed by linear combinations of the averaged source terms, i.e., temperature gradients and temperature differences involving mapping scalar and vectors that are given by a series of quasi-steady *closure* problems. As a consequence, the resulting effective

coefficients are not time dependent, and some historical effects are lost in this analysis. The implications of these assumptions have been studied on the basis of a comparison with numerical experiments [40,47,55,58], and these have shown that such two-equation models are satisfactory under a wide range of practical situations.

If one needs to incorporate in the analysis more transient phenomena, several possibilities are offered. Within the framework of two-equation models, transient effective properties may be used. Different ideas have been put forward, and they are discussed in some detail in [40,47]. The proposal by [47] involves transient closure problems. An alternate route has been proposed by [14], the resulting representation of the deviations is similar to the quasi-steady representation with additional terms involving time derivatives of the source terms. More advanced modelling of the transient behavior would require mixed models featuring one averaged equation for the high conductivity phase, coupled with a micro-scale equation for the low conductivity phase with a *mixed* boundary condition involving the averaged temperature on one side and the micro-scale temperature on the other side [4,5,8,26]. This approach would be extremely complex in practice since it would require fine gridding of one of the phase.

As a conclusion of this literature review, and given the complexity of the three-phase problem under consideration in this paper, we believe that the first attempt should follow the lines of the quasi-steady analysis. This theory has already been extended to the two-phase flow problem with convection [18,42,43,53,73] and with homogeneous and heterogeneous heat sources [61]. It has been also applied to the three-phase flow problem without phase change [52].

First, we simplify the transport equations for $\widetilde{T}_{\mathrm{g}}$ and $\widetilde{T}_{\ell}$ by making the assumption that the interface evolution at the pore level is quasi-static. Such an assumption is classically made for pore-scale moving boundary problems [20,57,60] and it basically means that velocities and interfaces are stationary at the pore-scale compared to other relaxation times. In addition, we make the assumption that the mass rate of evaporation has a negligible impact on the temperature deviations and as a result it is discarded in the governing equation for both $\widetilde{T}_{\mathrm{g}}$, Eq. (38), and $\widetilde{T}_{\ell}$. This assumption as well as the quasi-static description will be partially discussed in Section 7. Finally, we simplify the governing equations for the deviations by imposing the following constraints so that the $\widetilde{T}_{\mathrm{g}}$, $\widetilde{T}_{\ell}$ and $\widetilde{T}_{\mathrm{s}}$-fields can be treated as quasi-steady

$$\frac{k_{\mathrm{g}}t^*}{(\rho C_p)_{\mathrm{g}}\ell_{\mathrm{g}}^2}\gg 1,\quad \frac{k_{\ell}t^*}{(\rho C_p)_{\ell}\ell_{\ell}^2}\gg 1,\quad \frac{k_{\mathrm{s}}t^*}{(\rho C_p)_{\mathrm{s}}\ell_{\mathrm{s}}^2}\gg 1 \tag{39}$$

in which t^* is the characteristic process time. Under these circumstances, one can discard the temporal derivatives at the closure level. These constraints as well as their impact are discussed in detail in [53,55] for two-phase systems and here it will be assumed that they are satisfied for the three-phase system under consideration. Under these circumstances, the pore-scale boundary value problem for the deviations simplifies to

$$(\rho C_p)_{\mathrm{g}}\mathbf{v}_{\mathrm{g}}\cdot\nabla\widetilde{T}_{\mathrm{g}}+\underbrace{(\rho C_p)_{\mathrm{g}}\widetilde{\mathbf{v}}_{\mathrm{g}}\cdot\nabla\langle T_{\mathrm{g}}\rangle^{\mathrm{g}}}_{\text{source}}=\nabla\cdot(k_{\mathrm{g}}\nabla\widetilde{T}_{\mathrm{g}})$$
$$-\varepsilon_{\mathrm{g}}^{-1}\left(\frac{1}{V}\int_{A_{\mathrm{g}\ell}}\mathbf{n}_{\mathrm{g}\ell}\cdot k_{\mathrm{g}}\nabla\widetilde{T}_{\mathrm{g}}\,\mathrm{d}A+\frac{1}{V}\int_{A_{\mathrm{gs}}}\mathbf{n}_{\mathrm{gs}}\cdot k_{\mathrm{g}}\nabla\widetilde{T}_{\mathrm{g}}\,\mathrm{d}A\right),\quad\text{in the g-phase} \tag{40}$$

$$\widetilde{T}_{\mathrm{g}}=\underbrace{T^{\mathrm{sat}}-\langle T_{\mathrm{g}}\rangle^{\mathrm{g}}}_{\text{source}},\quad\text{at } A_{\ell\mathrm{g}} \tag{41}$$

$$\widetilde{T}_{\mathrm{g}}=\widetilde{T}_{\mathrm{s}}-\underbrace{(\langle T_{\mathrm{g}}\rangle^{\mathrm{g}}-T^{\mathrm{sat}})}_{\text{source}}+\underbrace{(\langle T_{\mathrm{s}}\rangle^{\mathrm{s}}-T^{\mathrm{sat}})}_{\text{source}},\quad\text{at } A_{\mathrm{gs}} \tag{42}$$

$$\mathbf{n}_{\mathrm{gs}}\cdot k_{\mathrm{g}}\nabla\widetilde{T}_{\mathrm{g}}=\mathbf{n}_{\mathrm{gs}}\cdot k_{\mathrm{s}}\nabla\widetilde{T}_{\mathrm{s}}-\underbrace{\mathbf{n}_{\mathrm{gs}}\cdot k_{\mathrm{g}}\nabla\langle T_{\mathrm{g}}\rangle^{\mathrm{g}}}_{\text{source}}+\underbrace{\mathbf{n}_{\mathrm{gs}}\cdot k_{\mathrm{s}}\nabla\langle T_{\mathrm{s}}\rangle^{\mathrm{s}}}_{\text{source}},\quad\text{at } A_{\mathrm{gs}} \tag{43}$$

$$(\rho C_p)_{\ell}\mathbf{v}_{\ell}\cdot\nabla\widetilde{T}_{\ell}+\underbrace{(\rho C_p)_{\ell}\widetilde{\mathbf{v}}_{\ell}\cdot\nabla\langle T_{\ell}\rangle^{\ell}}_{\text{source}}=\nabla\cdot(k_{\ell}\nabla\widetilde{T}_{\ell})$$
$$-\varepsilon_{\ell}^{-1}\left(\frac{1}{V}\int_{A_{\ell\mathrm{g}}}\mathbf{n}_{\ell\mathrm{g}}\cdot k_{\ell}\nabla\widetilde{T}_{\ell}\,\mathrm{d}A+\frac{1}{V}\int_{A_{\ell\mathrm{s}}}\mathbf{n}_{\ell\mathrm{s}}\cdot k_{\ell}\nabla\widetilde{T}_{\ell}\,\mathrm{d}A\right),\quad\text{in the }\ell\text{-phase} \tag{44}$$

$$\widetilde{T}_{\ell}=\underbrace{T^{\mathrm{sat}}-\langle T_{\ell}\rangle^{\ell}}_{\text{source}},\quad\text{at } A_{\ell\mathrm{g}} \tag{45}$$

$$\widetilde{T}_{\ell}=\widetilde{T}_{\mathrm{s}}+\underbrace{(\langle T_{\mathrm{s}}\rangle^{\mathrm{s}}-T^{\mathrm{sat}})}_{\text{source}}-\underbrace{(\langle T_{\ell}\rangle^{\ell}-T^{\mathrm{sat}})}_{\text{source}},\quad\text{at } A_{\ell\mathrm{s}} \tag{46}$$

$$\mathbf{n}_{\ell\mathrm{s}}\cdot k_{\ell}\nabla\widetilde{T}_{\ell}=\mathbf{n}_{\ell\mathrm{s}}\cdot k_{\mathrm{s}}\nabla\widetilde{T}_{\mathrm{s}}+\underbrace{\mathbf{n}_{\ell\mathrm{s}}\cdot k_{\mathrm{s}}\nabla\langle T_{\mathrm{s}}\rangle^{\mathrm{s}}}_{\text{source}}-\underbrace{\mathbf{n}_{\ell\mathrm{s}}\cdot k_{\ell}\nabla\langle T_{\ell}\rangle^{\ell}}_{\text{source}},\quad\text{at } A_{\ell\mathrm{s}} \tag{47}$$

$$0=\nabla\cdot(k_{\mathrm{s}}\nabla\widetilde{T}_{\mathrm{s}})$$
$$-\varepsilon_{\mathrm{s}}^{-1}\left(\frac{1}{V}\int_{A_{\mathrm{s}\ell}}\mathbf{n}_{\mathrm{s}\ell}\cdot k_{\mathrm{s}}\nabla\widetilde{T}_{\mathrm{s}}\,\mathrm{d}A+\frac{1}{V}\int_{A_{\mathrm{sg}}}\mathbf{n}_{\mathrm{sg}}\cdot k_{\mathrm{s}}\nabla\widetilde{T}_{\mathrm{s}}\,\mathrm{d}A\right),\quad\text{in the s-phase} \tag{48}$$

Here we have decomposed the boundary conditions in a convenient form in order to introduce the phase change temperature. In this problem, we have identified six terms as macroscopic source terms since they act as generators of the spatial deviation temperatures [61]. Given the six sources in the closure problem, we can follow previous studies [18,53,55,73] and the above dis-

cussion to express the spatial deviation temperatures in terms of the macroscopic source terms according to the following linear representation

$$\widetilde{T}_{\mathrm{g}} = -s^{\mathrm{g}}_{\ell\mathrm{i}}(\langle T_\ell\rangle^{\ell} - T^{\mathrm{sat}}) - s^{\mathrm{g}}_{\mathrm{gi}}(\langle T_{\mathrm{g}}\rangle^{\mathrm{g}} - T^{\mathrm{sat}}) - s^{\mathrm{g}}_{\mathrm{si}}(\langle T_{\mathrm{s}}\rangle^{\mathrm{s}} - T^{\mathrm{sat}}) + \mathbf{b}_{\mathrm{g}\ell}\cdot\nabla\langle T_\ell\rangle^{\ell} + \mathbf{b}_{\mathrm{gg}}\cdot\nabla\langle T_{\mathrm{g}}\rangle^{\mathrm{g}} + \mathbf{b}_{\mathrm{gs}}\cdot\nabla\langle T_{\mathrm{s}}\rangle^{\mathrm{s}} \tag{49}$$

$$\widetilde{T}_{\ell} = -s^{\ell}_{\ell\mathrm{i}}(\langle T_\ell\rangle^{\ell} - T^{\mathrm{sat}}) - s^{\ell}_{\mathrm{gi}}(\langle T_{\mathrm{g}}\rangle^{\mathrm{g}} - T^{\mathrm{sat}}) - s^{\ell}_{\mathrm{si}}(\langle T_{\mathrm{s}}\rangle^{\mathrm{s}} - T^{\mathrm{sat}}) + \mathbf{b}_{\ell\ell}\cdot\nabla\langle T_\ell\rangle^{\ell} + \mathbf{b}_{\ell\mathrm{g}}\cdot\nabla\langle T_{\mathrm{g}}\rangle^{\mathrm{g}} + \mathbf{b}_{\ell\mathrm{s}}\cdot\nabla\langle T_{\mathrm{s}}\rangle^{\mathrm{s}} \tag{50}$$

$$\widetilde{T}_{\mathrm{s}} = -s^{\mathrm{s}}_{\ell\mathrm{i}}(\langle T_\ell\rangle^{\ell} - T^{\mathrm{sat}}) - s^{\mathrm{s}}_{\mathrm{gi}}(\langle T_{\mathrm{g}}\rangle^{\mathrm{g}} - T^{\mathrm{sat}}) - s^{\mathrm{s}}_{\mathrm{si}}(\langle T_{\mathrm{s}}\rangle^{\mathrm{s}} - T^{\mathrm{sat}}) + \mathbf{b}_{\mathrm{s}\ell}\cdot\nabla\langle T_\ell\rangle^{\ell} + \mathbf{b}_{\mathrm{sg}}\cdot\nabla\langle T_{\mathrm{g}}\rangle^{\mathrm{g}} + \mathbf{b}_{\mathrm{ss}}\cdot\nabla\langle T_{\mathrm{s}}\rangle^{\mathrm{s}} \tag{51}$$

The variables $s^{\mathrm{s}}_{\ell\mathrm{i}}$, $\mathbf{b}_{\mathrm{s}\ell}$, etc., are the closure variables or the mapping variables that realize an *approximate solution of the coupled equations*. We remind the reader that in doing so we have neglected in the analysis possible transient phenomena as well as second order terms in the above expansions, and numerical experiments will be required to test the applicability of the given approximations. A limited validation will be proposed later in this paper in the case of purely diffusive problems. The nomenclature used for the mapping scalars is such that the superscript always identifies the phase in which the function is defined, while the subscript always indicates which temperature difference is being mapped onto a spatial deviation. For example, $s^{\mathrm{s}}_{\ell\mathrm{i}}$ refers to the scalar field that maps $(\langle T_\ell\rangle^{\ell} - T^{\mathrm{sat}})$ onto $\widetilde{T}_{\mathrm{s}}$ where the subscript 'i' refers to the interface temperature T^{sat}. For the mapping vectors, the first subscript always identifies the phase in which the function is defined, while the second subscript always indicates which temperature gradient is being mapped onto a spatial deviation. For example, $\mathbf{b}_{\mathrm{s}\ell}$ refers to the vector field that maps $\nabla\langle T_\ell\rangle^{\ell}$ onto $\widetilde{T}_{\mathrm{s}}$.

The closure variables are solution of six pore-scale boundary value problems, the so-called closure problems, which are given in appendix. When solving the closure problems, it is assumed that the porous medium can be represented by a periodic system as shown in Fig. 2. In this case, the period stands for the averaging volume and closure problems have to be solved over representative unit cells of the three-phase system under consideration with periodic boundary conditions. The interested reader is referred to [53,55] for a full discussion about the use of periodic unit cells and its validity regarding ordered and disordered systems.

It is important to keep in mind that the quasi-steady assumption implies that the closure variables, and the effective properties are calculated for different, *arbitrary* velocity fields and interface topology but do not take into account the historical evolution of liquid–vapor interfaces, for instance the effects of moving contact lines. Some history effects associated to transient diffusion can eventually be recovered with an unsteady closure as previously discussed (see for instance [47]) for two-phase systems in the purely diffusive case. Results of

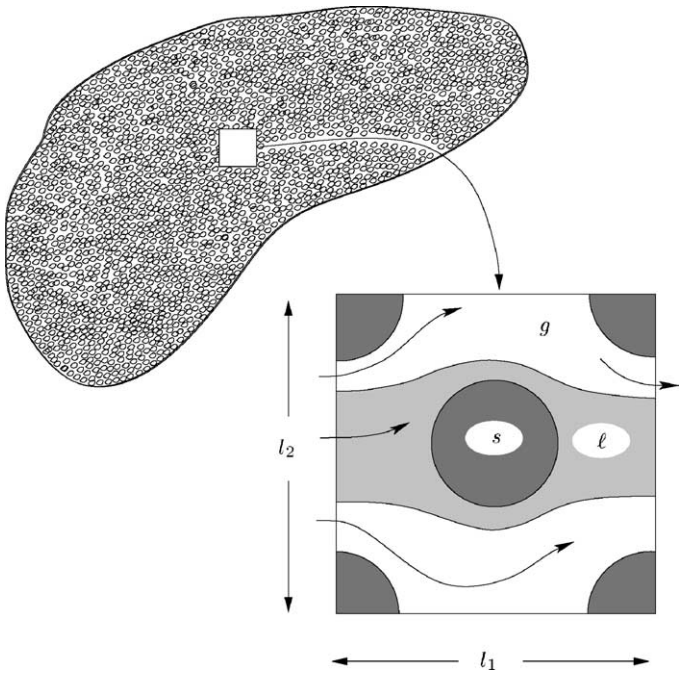

Fig. 2. Unit cell of a spatially periodic model of a porous medium.

this study indicate that the steady-state closure is sufficient, in most cases, in comparison to the more complicated case of the unsteady closure. Such a result cannot be applied directly to the three-phase systems with liquid–vapor phase change mainly because the two-phase flow problem is considerably much more complicated. Therefore, an extension to this work appears to be a challenging problem and seems to be premature. While we have discussed the historical effects associated with transient diffusion, we are now in a position to discuss the historical effects associated to the moving interfaces. Assuming the geometry of the interface at a given time fixes the volume fractions and the solution of the closure problems, i.e., the effective properties, which we will denote at this time as K_{eff}. The theory gives relationships such as

$$t \to \begin{cases} \varepsilon_\ell(t), \dots \\ K_{\text{eff}}(t), \dots \end{cases} \tag{52}$$

and this is not equivalent to

$$K_{\text{eff}} = K_{\text{eff}}(\varepsilon_\ell, \dots) \tag{53}$$

which would give a fully closed theory. In principle, different history of the interface evolution may lead to the same volume fractions with very different effective properties values. This important effect must be checked in future developments. At this time, we will remember that the functional dependence $K_{\text{eff}} = K_{\text{eff}}(\varepsilon_\ell, \dots)$ we may construct is entirely associated to the assumption made for the phases repartition.

5. Closed form of the averaged equations

Given the representations Eqs. (49)–(51), we are now in a position to obtain a closed form of the macroscopic transport equations (34)–(36). For the g-phase, use of the representation for $\widetilde{T}_{\text{g}}$ Eq. (49) in the volume averaged equation (34), leads to the following closed form

$$\begin{aligned}
&\varepsilon_{\text{g}}(\rho C_p)_{\text{g}} \frac{\partial \langle T_{\text{g}} \rangle^{\text{g}}}{\partial t} + (\rho C_p)_{\text{g}} \langle \mathbf{v}_{\text{g}} \rangle \cdot \nabla \langle T_{\text{g}} \rangle^{\text{g}} \\
&\quad - \nabla \cdot [\mathbf{d}^{\text{g}}_{\ell\text{i}} (\langle T_\ell \rangle^{\ell} - T^{\text{sat}})] - \nabla \cdot [\mathbf{d}^{\text{g}}_{\text{gi}} (\langle T_{\text{g}} \rangle^{\text{g}} - T^{\text{sat}})] \\
&\quad - \nabla \cdot [\mathbf{d}^{\text{g}}_{\text{si}} (\langle T_{\text{s}} \rangle^{\text{s}} - T^{\text{sat}})] - \mathbf{u}_{\text{gg}} \cdot \nabla \langle T_{\text{g}} \rangle^{\text{g}} - \mathbf{u}_{\text{g}\ell} \cdot \nabla \langle T_\ell \rangle^{\ell} \\
&\quad - \mathbf{u}_{\text{gs}} \cdot \nabla \langle T_{\text{s}} \rangle^{\text{s}} \\
&\quad = \nabla \cdot (\mathbf{K}_{\text{gg}} \cdot \nabla \langle T_{\text{g}} \rangle^{\text{g}} + \mathbf{K}_{\text{g}\ell} \cdot \nabla \langle T_\ell \rangle^{\ell} + \mathbf{K}_{\text{gs}} \cdot \nabla \langle T_{\text{s}} \rangle^{\text{s}}) \\
&\qquad - \nabla \varepsilon_{\text{g}} \cdot k_{\text{g}} \nabla \langle T_{\text{g}} \rangle^{\text{g}} - \dot{m} C_{p\text{g}} (\langle T_{\text{g}} \rangle^{\text{g}} - T^{\text{sat}}) \\
&\qquad - (h^{\text{g}\ell}_{\ell\text{i}} + h^{\text{gs}}_{\ell\text{i}})(\langle T_\ell \rangle^{\ell} - T^{\text{sat}}) - (h^{\text{g}\ell}_{\text{gi}} + h^{\text{gs}}_{\text{gi}})(\langle T_{\text{g}} \rangle^{\text{g}} - T^{\text{sat}}) \\
&\qquad - (h^{\text{g}\ell}_{\text{si}} + h^{\text{gs}}_{\text{si}})(\langle T_{\text{s}} \rangle^{\text{s}} - T^{\text{sat}})
\end{aligned} \tag{54}$$

In this equation, the effective transport coefficients such as $\mathbf{K}_{\text{gg}}$, $h^{\text{g}\ell}_{\ell\text{i}}$, etc., are related to the pore-scale physics through the six closure problems given in appendix. The definitions of these coefficients are also reported in appendix. $\mathbf{K}_{\text{gg}}$, $\mathbf{K}_{\text{g}\ell}$ and $\mathbf{K}_{\text{gs}}$ refer to the effective thermal dispersion tensors. They have a contribution from both conduction and hydrodynamic dispersion, and are defined by Eqs. (B.1)–(B.3). It must be noticed that the expressions for the thermal dispersion tensors take explicitly into account the boundary conditions at the liquid–vapor interface that appear in the closure problems. The thermal dispersion tensor $\mathbf{K}_{\text{gg}}$ is referred to as the dominant thermal dispersion tensor while $\mathbf{K}_{\text{g}\ell}$ and $\mathbf{K}_{\text{gs}}$ are referred to as the coupling thermal dispersion tensors [61]. In Eqs. (B.2) and (B.3) given in appendix, the first two terms represent contribution from tortuosity while the last term represents the hydrodynamic thermal dispersion contribution. The dominant thermal dispersion tensor has an additional contribution from thermal diffusion represented by the first term in Eq. (B.1). Because their form is similar to the traditional macroscopic convective term, the three transport coefficients $\mathbf{u}_{\text{gg}}$, $\mathbf{u}_{\text{g}\ell}$ and $\mathbf{u}_{\text{gs}}$ in Eq. (54) are called velocity-like coefficients and are defined from closure problems IV, V, VI by Eqs. (B.10)–(B.12). The other effective properties are characteristic of non-equilibrium models [18,53,55,73]. The three effective coefficients $\mathbf{d}^{\text{g}}_{\ell\text{i}}$, $\mathbf{d}^{\text{g}}_{\text{gi}}$ and $\mathbf{d}^{\text{g}}_{\text{si}}$ represent the so-called additional velocity-like coefficients and are defined by Eqs. (B.13)–(B.15). Here again, these coefficients are defined in accordance with the boundary conditions at the closure level. The others coefficients that appear in Eq. (54) $h^{\text{g}\ell}_{\ell\text{i}}$, etc., are the heat transfer coefficients and are defined directly from closure problems I, II, III. Equations analogous to Eq. (54) describe the intrinsic phase average temperatures for the ℓ-phase and the s-phase, and these equations are given by

$$\begin{aligned}
&\varepsilon_\ell(\rho C_p)_\ell \frac{\partial \langle T_\ell \rangle^{\ell}}{\partial t} + \varepsilon_\ell(\rho C_p)_\ell \langle \mathbf{v}_\ell \rangle^{\ell} \cdot \nabla \langle T_\ell \rangle^{\ell} \\
&\quad - \nabla \cdot [\mathbf{d}^{\ell}_{\ell\text{i}} (\langle T_\ell \rangle^{\ell} - T^{\text{sat}})] - \nabla \cdot [\mathbf{d}^{\ell}_{\text{gi}} (\langle T_{\text{g}} \rangle^{\text{g}} - T^{\text{sat}})] \\
&\quad - \nabla \cdot [\mathbf{d}^{\ell}_{\text{si}} (\langle T_{\text{s}} \rangle^{\text{s}} - T^{\text{sat}})] - \mathbf{u}_{\ell\text{g}} \cdot \nabla \langle T_{\text{g}} \rangle^{\text{g}} - \mathbf{u}_{\ell\ell} \cdot \nabla \langle T_\ell \rangle^{\ell} \\
&\quad - \mathbf{u}_{\ell\text{s}} \cdot \nabla \langle T_{\text{s}} \rangle^{\text{s}} \\
&\quad = \nabla \cdot (\mathbf{K}_{\ell\text{g}} \cdot \nabla \langle T_{\text{g}} \rangle^{\text{g}} + \mathbf{K}_{\ell\ell} \cdot \nabla \langle T_\ell \rangle^{\ell} + \mathbf{K}_{\ell\text{s}} \cdot \nabla \langle T_{\text{s}} \rangle^{\text{s}}) \\
&\qquad - \nabla \varepsilon_\ell \cdot k_\ell \nabla \langle T_\ell \rangle^{\ell} + \dot{m} C_{p\ell} (\langle T_\ell \rangle^{\ell} - T^{\text{sat}}) \\
&\qquad - (h^{\ell\text{g}}_{\ell\text{i}} + h^{\ell\text{s}}_{\ell\text{i}})(\langle T_\ell \rangle^{\ell} - T^{\text{sat}}) - (h^{\ell\text{g}}_{\text{gi}} + h^{\ell\text{s}}_{\text{gi}})(\langle T^{\text{g}}_{\text{g}} \rangle - T^{\text{sat}}) \\
&\qquad - (h^{\ell\text{g}}_{\text{si}} + h^{\ell\text{s}}_{\text{si}})(\langle T_{\text{s}} \rangle^{\text{s}} - T^{\text{sat}})
\end{aligned} \tag{55}$$

$$\begin{aligned}
&\varepsilon_{\text{s}}(\rho C_p)_{\text{s}} \frac{\partial \langle T_{\text{s}} \rangle^{\text{s}}}{\partial t} - \nabla \cdot [\mathbf{d}^{\text{s}}_{\ell\text{i}} (\langle T_\ell \rangle^{\ell} - T^{\text{sat}})] \\
&\quad - \nabla \cdot [\mathbf{d}^{\text{s}}_{\text{gi}} (\langle T_{\text{g}} \rangle^{\text{g}} - T^{\text{sat}})] - \nabla \cdot [\mathbf{d}^{\text{s}}_{\text{si}} (\langle T_{\text{s}} \rangle^{\text{s}} - T^{\text{sat}})] \\
&\quad - \mathbf{u}_{\text{sg}} \cdot \nabla \langle T_{\text{g}} \rangle^{\text{g}} - \mathbf{u}_{\text{s}\ell} \cdot \nabla \langle T_\ell \rangle^{\ell} - \mathbf{u}_{\text{ss}} \cdot \nabla \langle T_{\text{s}} \rangle^{\text{s}} \\
&\quad = \nabla \cdot (\mathbf{K}_{\text{sg}} \cdot \nabla \langle T_{\text{g}} \rangle^{\text{g}} + \mathbf{K}_{\text{s}\ell} \cdot \nabla \langle T_\ell \rangle^{\ell} + \mathbf{K}_{\text{ss}} \cdot \nabla \langle T_{\text{s}} \rangle^{\text{s}}) \\
&\qquad - \nabla \varepsilon_{\text{s}} \cdot k_{\text{s}} \nabla \langle T_{\text{s}} \rangle^{\text{s}} - (h^{\text{s}\ell}_{\ell\text{i}} + h^{\text{sg}}_{\ell\text{i}})(\langle T_\ell \rangle^{\ell} - T^{\text{sat}}) \\
&\qquad - (h^{\text{s}\ell}_{\text{gi}} + h^{\text{sg}}_{\text{gi}})(\langle T_{\text{g}} \rangle^{\text{g}} - T^{\text{sat}}) - (h^{\text{s}\ell}_{\text{si}} + h^{\text{sg}}_{\text{si}})(\langle T_{\text{s}} \rangle^{\text{s}} - T^{\text{sat}}) \\
&\qquad + \varepsilon_{\text{s}} \langle \varpi_{\text{s}} \rangle^{\text{s}}
\end{aligned} \tag{56}$$

Compared to the traditional heuristic models, the coupling between the three equations appears to be much more complex not only because of the distribution of inter-continuum heat fluxes but also because of additional diffusion-like and convective-like coupling terms. We expect thermal dispersion tensors and heat exchange coefficients to be the dominant contributions in Eqs. (54)–(56). Analytical expressions for the additional convective terms are given in appendix in the case of a simple stratified unit cell and results show that the longitudinal components have a negligible contribution compared to the traditional term $\langle \mathbf{v}_g \rangle \cdot \nabla \langle T_g \rangle^g$ as was observed in [57]. However it is not clear whether these additional convective terms are of some importance in practical cases. For two-phase materials, Zhang and Huang [74] have calculated analytically these terms for two simplified unit cells and have studied their impact in a two-equation model. It is shown that the effects of the additional convective terms may be important or insignificant depending on the unit cell considered and the authors conclude that the importance of these terms remains to be examined for more complex unit cells. On the other hand, Quintard et al. [53] have calculated numerically the closure problems associated with a two-equation description for two and three-dimensional unit cells. The results indicate that the non-traditional terms might be important for a limited range of the cell Péclet numbers. The closure problems IV, V, VI given in appendix provide a framework to determine the velocity-like coefficients that appear in the three-equation model but in this paper we follow [52] and we assume that the additional convective terms do not play a very important role in the heat transfer process. If we adopt this simplification, the three-equation model may be written as

$$\begin{aligned}
&\varepsilon_g(\rho C_p)_g \frac{\partial \langle T_g \rangle^g}{\partial t} + (\rho C_p)_g \langle \mathbf{v}_g \rangle \cdot \nabla \langle T_g \rangle^g \\
&\quad = \nabla \cdot (\mathbf{K}_{gg} \cdot \nabla \langle T_g \rangle^g + \mathbf{K}_{g\ell} \cdot \nabla \langle T_\ell \rangle^\ell + \mathbf{K}_{gs} \cdot \nabla \langle T_s \rangle^s) \\
&\qquad - \nabla \varepsilon_g \cdot k_g \nabla \langle T_g \rangle^g - \dot{m} C_{pg} (\langle T_g \rangle^g - T^{sat}) \\
&\qquad - (h^{g\ell}_{\ell i} + h^{gs}_{\ell i})(\langle T_\ell \rangle^\ell - T^{sat}) - (h^{g\ell}_{gi} + h^{gs}_{gi})(\langle T_g \rangle^g - T^{sat}) \\
&\qquad - (h^{g\ell}_{si} + h^{gs}_{si})(\langle T_s \rangle^s - T^{sat}) \qquad (57)
\end{aligned}$$

$$\begin{aligned}
&\varepsilon_\ell(\rho C_p)_\ell \frac{\partial \langle T_\ell \rangle^\ell}{\partial t} + (\rho C_p)_\ell \langle \mathbf{v}_\ell \rangle \cdot \nabla \langle T_\ell \rangle^\ell \\
&\quad = \nabla \cdot (\mathbf{K}_{\ell g} \cdot \nabla \langle T_g \rangle^g + \mathbf{K}_{\ell\ell} \cdot \nabla \langle T_\ell \rangle^\ell + \mathbf{K}_{\ell s} \cdot \nabla \langle T_s \rangle^s) \\
&\qquad - \nabla \varepsilon_\ell \cdot k_\ell \nabla \langle T_\ell \rangle^\ell + \dot{m} C_{p\ell} (\langle T_\ell \rangle^\ell - T^{sat}) \\
&\qquad - (h^{\ell g}_{\ell i} + h^{\ell s}_{\ell i})(\langle T_\ell \rangle^\ell - T^{sat}) - (h^{\ell g}_{gi} + h^{\ell s}_{gi})(\langle T_g \rangle^g - T^{sat}) \\
&\qquad - (h^{\ell g}_{si} + h^{\ell s}_{si})(\langle T_s \rangle^s - T^{sat}) \qquad (58)
\end{aligned}$$

$$\begin{aligned}
&\varepsilon_s(\rho C_p)_s \frac{\partial \langle T_s \rangle^s}{\partial t} \\
&\quad = \nabla \cdot (\mathbf{K}_{sg} \cdot \nabla \langle T_g \rangle^g + \mathbf{K}_{s\ell} \cdot \nabla \langle T_\ell \rangle^\ell + \mathbf{K}_{ss} \cdot \nabla \langle T_s \rangle^s) \\
&\qquad - \nabla \varepsilon_s \cdot k_s \nabla \langle T_s \rangle^s - (h^{s\ell}_{\ell i} + h^{sg}_{\ell i})(\langle T_\ell \rangle^\ell - T^{sat}) \\
&\qquad - (h^{s\ell}_{gi} + h^{sg}_{gi})(\langle T_g \rangle^g - T^{sat}) - (h^{s\ell}_{si} + h^{sg}_{si})(\langle T_s \rangle^s - T^{sat}) \\
&\qquad + \varepsilon_s \langle \varpi_s \rangle^s \qquad (59)
\end{aligned}$$

We recall that Eqs. (57)–(59) constitute a simplified form of the three-equation model where it has been assumed that the non-traditional convective terms have a negligible impact on the macroscopic heat transfer process. At this point, the main difference between Eqs. (57)–(59) and the traditional three-equation models appears through the crossing thermal dispersion tensors. From a practical point of view, it is often assumed that the diffusive terms can be lumped into a single term in each transport equation, for instance for the g-phase:

$$\mathbf{K}_{gg} \cdot \nabla \langle T_g \rangle^g + \mathbf{K}_{g\ell} \cdot \nabla \langle T_\ell \rangle^\ell + \mathbf{K}_{gs} \cdot \nabla \langle T_s \rangle^s \simeq \mathbf{K}^*_g \cdot \nabla \langle T_g \rangle^g \qquad (60)$$

This assumption greatly simplifies the numerical treatment of the coupled macroscopic transport equations and is largely used in practical applications of two and three-equation models. The simplification represented by Eq. (60) is obviously valid when the macroscopic temperature gradients are sufficiently close to each other. Such a condition, referred to as local gradient equilibrium [58], is rather difficult to evaluate. It has been shown for a two-equation description [55] that the diffusive lumping Eq. (60) represents a good approximation for macroscopic one-dimensional problems but it is beyond the scope of this paper to repeat the analysis for the three-equation model.

6. Closed form of the mass rate of evaporation

We recall that the liquid–vapor interface temperature is fixed at the equilibrium saturation temperature and thus the boundary condition, Eq. (12), is an auxiliary condition that can be useful to determine the mass rate of evaporation. Using the mass balance equation (3), we first arrange the enthalpy jump condition Eq. (12) as

$$\mathbf{n}_{g\ell} \cdot \rho_g (h_g - h_\ell)(\mathbf{v}_g - \mathbf{w}) = \mathbf{n}_{g\ell} \cdot (k_g \nabla T_g - k_\ell \nabla T_\ell), \quad \text{at } A_{\ell g} \qquad (61)$$

We focus on the left-hand side of Eq. (61) and we introduce the point enthalpy–temperature relationships (26) and (27) using the boundary conditions Eq. (11), this leads to

$$\mathbf{n}_{g\ell} \cdot \rho_g (h_g - h_\ell)(\mathbf{v}_g - \mathbf{w}) = \mathbf{n}_{g\ell} \cdot \rho_g \Delta h (\mathbf{v}_g - \mathbf{w}), \quad \text{at } A_{\ell g} \qquad (62)$$

where $\Delta h = h_{\mathrm{g}}^{\mathrm{sat}} - h_{\ell}^{\mathrm{sat}}$ represents the latent heat of vaporization. Using this result and ignoring variations of Δh within the averaging volume, the mass rate of evaporation definition Eq. (17) allows to express the area average of the left-hand side of Eq. (61) as

$$\frac{1}{V}\int_{A_{\mathrm{g}\ell}} \mathbf{n}_{\mathrm{g}\ell}\cdot\rho_{\mathrm{g}}(h_{\mathrm{g}}-h_{\ell})(\mathbf{v}_{\mathrm{g}}-\mathbf{w})\,\mathrm{d}A = -\dot{m}\Delta h \tag{63}$$

At this point, we have developed the auxiliary condition Eq. (12) to obtain the following expression for the mass rate of evaporation at the macroscopic level

$$\dot{m}\Delta h = \frac{1}{V}\int_{A_{\mathrm{g}\ell}} \mathbf{n}_{\mathrm{g}\ell}\cdot(k_{\ell}\nabla T_{\ell} - k_{\mathrm{g}}\nabla T_{\mathrm{g}})\,\mathrm{d}A \tag{64}$$

This result clearly indicates that the determination of the phase change rate $\dot{m}$ is equivalent to the calculation of heat transfers between fluid phases.

When using a thermal equilibrium model, the situation is quite different. The assumption of thermal equilibrium is rather useful, even though it cannot exist strictly. Heat transfers between the phases are assumed to be infinitely fast compared to other phenomena. When local thermal equilibrium is assumed to be valid, the three-phase system can be described by a single spatial average temperature $\langle T\rangle$ and the following approximation can be used $\langle T\rangle \simeq \langle T_{\mathrm{g}}\rangle^{\mathrm{g}} \simeq \langle T_{\ell}\rangle^{\ell} \simeq \langle T_{\mathrm{s}}\rangle^{\mathrm{s}}$. Particularly, when phase change occurs in a single-component three-phase system, the thermodynamic equilibrium condition Eq. (11) implies that the two-phase region is nearly isothermal, that is $\langle T\rangle \simeq T^{\mathrm{sat}}$. As a consequence, the thermal energy equation is replaced by an equation for the liquid volume fraction in the two-phase region while the energy equation represents a temperature equation in the single fluid phases. Such a formulation has been proposed by Wang and Beckerman [65] on the basis of the so-called two-phase mixture model. For steady one-dimensional two-phase flow induced by volumetric heating, this model reduces to the Lipinski model [45] which has been extensively used to study debris bed coolability in the framework of severe nuclear reactor accidents analysis. For such a model, the energy equation reduces to $\dot{m} = \langle\varpi_{\mathrm{s}}\rangle/\Delta h$ in the isothermal two-phase region, while $\dot{m} = 0$ must be specified for $\langle T\rangle \neq T^{\mathrm{sat}}$ in the single fluid phases to describe for instance post-dryout heat transfer [22].

In the case of a two-temperature model, it is generally assumed that both liquid and vapor phases can be described in terms of a single *fluid average* temperature $\langle T_{\mathrm{f}}\rangle^{\mathrm{f}}$ [63] such as $\langle T_{\mathrm{f}}\rangle^{\mathrm{f}} \simeq \langle T_{\mathrm{g}}\rangle^{\mathrm{g}} \simeq \langle T_{\ell}\rangle^{\ell}$, that is local thermal equilibrium between fluid phases. In this case, owing to the thermodynamic equilibrium condition, one has again during phase change $\langle T_{\mathrm{f}}\rangle^{\mathrm{f}} \simeq T^{\mathrm{sat}}$. A similar development as for the one-temperature model allows to simplify the fluid energy equation in the two-phase region as $\dot{m}\Delta h = h_{\mathrm{fs}}(\langle T_{\mathrm{s}}\rangle^{\mathrm{s}} - T^{\mathrm{sat}})$ where h_{fs} is the fluid to solid heat transfer coefficient. It must be kept in mind that this expression applies only to regions where both the liquid and vapor volume fractions are non-zero and once again $\dot{m}$ must be set to zero in the single fluid phases when $\langle T_{\mathrm{s}}\rangle^{\mathrm{s}} \neq T^{\mathrm{sat}}$ in the case of a constant heat transfer coefficient. This expression for the mass rate of evaporation has been used for instance by Décossin [25] within the framework of a heuristical *two-equation* model that does not make the local thermal equilibrium assumption but assumes that the liquid phase is nearly isothermal in equilibrium with the phase change temperature. In this sense, this model can be viewed as a three-temperature two-equation model. If one returns to traditional two-equation models, it must be noted that the two-temperature description cannot take into account overheating and undercooling of the fluid phases and also the associated evaporation and condensation respectively owing to the assumption $\langle T_{\mathrm{g}}\rangle^{\mathrm{g}} \simeq \langle T_{\ell}\rangle^{\ell}$. This contrasts with the use of a three-temperature description for which the heat flux to the fluid may have three different effects. This heat flux may indeed heat or cool both the vapor and the liquid phases and induce evaporation or condensation. Because of this, it is not possible to obtain a simple expression of the phase change rate as for one and two-temperature models. Some authors overcome this problem by considering only the two macroscopic continua associated with the fluid phases and, as a result, they propose the following form for the mass rate of evaporation [3,51]:

$$\dot{m}\Delta h = h_{\mathrm{gi}}(\langle T_{\mathrm{g}}\rangle^{\mathrm{g}} - T^{\mathrm{sat}}) + h_{\ell\mathrm{i}}(\langle T_{\ell}\rangle^{\ell} - T^{\mathrm{sat}}) \tag{65}$$

This relation is the simplest form that reflects the estimate of the right-hand side of Eq. (64) but indicates that heat transfers with the solid phase have a direct impact on the fluid temperatures and only an indirect impact on the evaporation rate. It appears as a particular case of a more general formulation which should take the form

$$\dot{m}\Delta h = h_{\mathrm{gi}}(\langle T_{\mathrm{g}}\rangle^{\mathrm{g}} - T^{\mathrm{sat}}) + h_{\ell\mathrm{i}}(\langle T_{\ell}\rangle^{\ell} - T^{\mathrm{sat}}) + h_{\mathrm{si}}(\langle T_{\mathrm{s}}\rangle^{\mathrm{s}} - T^{\mathrm{sat}}) \tag{66}$$

Such a formulation involving the three macroscopic driving temperature differences has been proposed by Berthoud and Valette [13] and Likhanski et al. [44] on the basis of a heuristic approach. In the approach proposed in these references, the expression for $\dot{m}$ is derived in a consistent manner with the non-equilibrium terms that appear in the macroscopic thermal energy transport equations. The problem comes from the distribution of the macroscopic heat flux between the three continua (i.e. h_{gi}, $h_{\ell\mathrm{i}}$ and h_{si}). It depends, as a first approximation, on the distribution of contact area and we refer to the introduction of this paper for the difficulties associated with the determination of macroscopic heat fluxes.

In this paper, we follow the same idea developed in [35,60] to obtain a closed form of the mass rate of

evaporation using the method of volume averaging. We recall that $\dot{m}$ is given by Eq. (64) and we now focus on the right-hand side of this relation. First, we decompose the point temperatures T_g and T_ℓ according to Eq. (14) using the representations for the spatial deviations temperatures $\widetilde{T}_g$ and $\widetilde{T}_\ell$ given by Eqs. (49) and (50). Then, from the definition of the effective transport coefficients, the right-hand side of Eq. (64) takes the form

$$\begin{aligned}\frac{1}{V}\int_{A_{g\ell}} \mathbf{n}_{g\ell}\cdot(k_\ell\nabla T_\ell - k_g\nabla T_g)\,dA &= \frac{1}{V}\int_{A_{g\ell}} \mathbf{n}_{g\ell}\,dA\cdot(k_\ell\nabla\langle T_\ell\rangle^\ell - k_g\nabla\langle T_g\rangle^g)\\ &\quad - (\mathbf{c}^{\ell g}_{\ell g} + \mathbf{c}^{g\ell}_{gg})\cdot\nabla\langle T_g\rangle^g - (\mathbf{c}^{\ell g}_{\ell\ell} + \mathbf{c}^{g\ell}_{g\ell})\cdot\nabla\langle T_\ell\rangle^\ell\\ &\quad - (\mathbf{c}^{\ell g}_{\ell s} + \mathbf{c}^{g\ell}_{gs})\cdot\nabla\langle T_s\rangle^s + (h^{\ell g}_{\ell i} + h^{g\ell}_{\ell i})(\langle T_\ell\rangle^\ell - T^{sat})\\ &\quad + (h^{\ell g}_{gi} + h^{g\ell}_{gi})(\langle T_g\rangle^g - T^{sat}) + (h^{\ell g}_{si} + h^{g\ell}_{si})(\langle T_s\rangle^s - T^{sat})\end{aligned} \tag{67}$$

After extensive use of the boundary conditions at the liquid–vapor interface that appear in closure problems I, II, III, IV, V, VI and from the definitions of the velocity-like coefficients, one can simplify this result and we finally arrive from Eqs. (64) and (67) at the following closed form of the mass rate of evaporation

$$\begin{aligned}\dot{m}\Delta h &= (k_g\nabla\varepsilon_g - \mathbf{u}^*_g)\cdot\nabla\langle T_g\rangle^g + (k_\ell\nabla\varepsilon_\ell - \mathbf{u}^*_\ell)\cdot\nabla\langle T_\ell\rangle^\ell\\ &\quad + (k_s\nabla\varepsilon_s - \mathbf{u}^*_s)\cdot\nabla\langle T_s\rangle^s + (h^{\ell g}_{\ell i} + h^{g\ell}_{\ell i})(\langle T_\ell\rangle^\ell - T^{sat})\\ &\quad + (h^{\ell g}_{gi} + h^{g\ell}_{gi})(\langle T_g\rangle^g - T^{sat}) + (h^{\ell g}_{si} + h^{g\ell}_{si})(\langle T_s\rangle^s - T^{sat})\end{aligned} \tag{68}$$

where we have adopted the following notations:

$$\mathbf{u}^*_g = \mathbf{u}_{\ell g} + \mathbf{u}_{gg} + \mathbf{u}_{sg},\quad \mathbf{u}^*_\ell = \mathbf{u}_{\ell\ell} + \mathbf{u}_{g\ell} + \mathbf{u}_{s\ell},\quad \mathbf{u}^*_s = \mathbf{u}_{\ell s} + \mathbf{u}_{gs} + \mathbf{u}_{ss} \tag{69}$$

One may notice that when the volume fraction gradients and the pseudo-convective contributions are negligible, the mass rate of evaporation given by Eq. (68) takes a form similar to those proposed in heuristic models.

7. Discussion

The three macro-scale equations, Eqs. (54)–(56), obtained from the volume averaging theory represent a generalized quasi-steady three-equation model for the macroscopic description of two-phase flow heat and mass transfer in porous media in the case of local thermal non-equilibrium. We recall here that the word quasi-steady refers to the fact that the effective transport coefficients depend on the physical properties as well as the pore-scale geometry but do not include some possible history effects. The methodology used to derive the macro-scale model has two important features. First, starting from the pore-scale description, the use of an up-scaling theory allows to clearly identify the main difficulties associated with the macro-scale description. The second feature that represents a great advantage of the method is to provide closure problems that give an explicit relationship between the lower scale and the upper scale. This allows to determine all the effective coefficients from the pore-scale description.

Regarding the difficulties associated with the macro-scale description, we first briefly recall below the main approximations that have led to the fully closed three-equation model.

1. First, assuming that the heat transfer problem could be decoupled from the two-phase flow problem, we have made the assumption that the flow was quasi-static meaning that liquid–vapor interfaces behave as stationary at the pore-scale.
2. Next, on the basis of the coupled equations formed by the macro-scale averaged equations and the micro-scale ones and neglecting the impact of the phase change rate, we have proposed a quasi-steady approximation which consists in representing the spatial deviations as a first order expansion of the macroscopic source terms.

Hence, it is clear at this point that the three-equation model has limitations which correspond to the approximations listed above and we present below some comments concerning the use of these approximations.

- While the quasi-static approximation may be physically relevant for some transport processes with phase change in porous media (see for instance [17]), it is obviously quite debatable for liquid–vapor systems especially for local thermal non-equilibrium situations. However, its impact on the quality of the macroscopic description still remains an open question. Indeed, as indicated in Section 2, the quasi-static approximation is fully consistent with the usual generalized Darcy's laws which produce nevertheless a satisfactory description of the macroscopic behavior over a large range of problems involving non-quasi-static conditions. A possible explanation would be a spatiotemporal ergodicity for which the spatial average over a given elementary volume containing a lot of interfaces would lead implicitly to a time average of the interface movements and as a result they would evolve as quasi-static. A complete analysis on the domain of validity of a quasi-static theory represents obviously an extremely challenging task. Here, we just note that, from a practical point of view, a quasi-static theory may produce satisfactory results even for situations involving non-quasi-static flows.

- When looking at the coupled problem for the averaged temperatures and deviations, even if the quasi-static approximation leads to important simplifications from the macro-scale description point of view, it must be noted that the phase change rate still remains at the closure level. This is clear when returning to the definition, Eq. (17), for the mass rate of evaporation and by noticing that even if the quasi-static approximation allows to neglect the impact of the speed of displacement of the interface, the liquid or vapor velocity at the liquid–vapor interface is not necessarily zero. At this time, we are not ready to examine the significance of the phase change rate at the closure level mainly because of a lack of quantitative data. Hence, we have decided here to neglect the impact of the phase change rate on the spatial deviations in order to obtain a first approximate solution of the coupled problem. We acknowledge that such a simplifying assumption may result in underestimated macro-scale heat transfers but we insist on the fact that this does not mean that the phase change rate is neglected at the macroscopic level.
- While we have discussed some inherent difficulties in multiphase up-scaling problems, we now turn to the quasi-steady approximation represented by Eqs. (49)–(51) which leads to the fully closed averaged equations. As previously discussed in Section 4, the quasi-steady description corresponds to a first order approximation of the mixed micro-scale macro-scale problem without accounting for memory effects. A direct consequence is that macro-scale heat exchanges between continua are written as the product of a constant heat transfer coefficient and a driving force represented by an averaged temperature difference. This rough description of the transient behavior is based on the fact that the spatial deviations in Eqs. (40)–(48) are assumed to evolve as quasi-steady in comparison to the averaged values. This is expressed by the constraints (39) involving a characteristic time of the process under consideration. Hence, a more thorough knowledge of this characteristic time is required to examine the validity of a quasi-steady description. Unfortunately, following previous developments conducted in a purely diffuse case [59], the validity of these constraints appears rather obscure. Furthermore, numerical experiments carried out for two-phase systems [58] have shown a strong impact of the pore-scale topology as well as phase repartition, impact which is difficult to take into account through some time or space characteristic scales. As a result, a general discussion about the validity of the constraints (39) is extremely difficult and, in most cases, the validity of a quasi-steady approximation is examined through pore-scale numerical simulations. In this work, we will follow the same approach and we will test the theory versus pore-scale numerical experiments.

Giving these approximations, the resulting macro-scale equations may be seen as a *generalization* of existing quasi-steady three-equation models obtained from a heuristic approach. As noticed in Section 5, the main differences are the existence of additional terms represented by diffusion-like and convection-like terms and a coupling between the macroscopic continua that seems to be more complex through cross-dispersion and cross-convection terms as well as macro-scale heat exchanges. One of the *attractive features* of the proposed three-equation model lies in the derivation of a *closed form of the evaporation rate* at the closure level without any additional phenomenological relation. This form has been obtained in a way which is fully consistent with the approximate solution proposed at the closure level and it is interesting to note that it exhibits some links with those proposed in heuristic models. Moreover, it can be shown [27] that this three-equation model is fully compatible with the two- and the one-equation models without any additional relations between the effective coefficients, especially the heat exchange coefficients. We recall here that the two-equation model refers generally to the one obtained when the fluid average temperatures, liquid and vapor, are assumed to be very close to each other. This corresponds to the most standard case but obviously other two-equation models can be obtained. Even if it is premature to perform a full comparison with the usual three-equation models, the proposed macro-scale description is certainly improved mainly because of the additional terms and a more complex coupling between the averaged equations. On the other hand, the price we have to pay for this improved description is the increased number of the effective transport coefficients. Here, a great advantage of the up-scaling theory lies in the possibility of determining all these coefficients from pore-scale characteristics through the solution of the six closure problems.

As indicated in Section 4, the closure problems have to be solved over a representative unit cell of the system under consideration. This unit cell should be as complex as needed to take into account as many informations as possible concerning the characterization of the system (e.g. matrix structure, liquid–vapor interfaces topology, two-phase flow regime, etc.). Dealing with very complex unit cells represent a very complicated task and goes beyond the scope of this paper. In order to perform a preliminary test of the theory, we present in this paper a study of relatively simple unit cells, which will provide first estimates of the effective properties. Moreover, we will see in the next section that it is rather easy for these simplified geometries to test the theory versus direct pore-scale simulations. Some results are presented in appendix for a stratified system and a capillary-like porous structure. The corresponding unit cells are

shown in Figs. 10 and 12 and are denoted as the stratified and the Chang's cells respectively. For such unit cells, two typical phases repartition may be considered, namely the s–ℓ–g and the s–g–ℓ repartitions. The first is classic for non-saturated media and refers to liquid being the wetting phase while the latter is more specific to boiling situations such as film boiling and refers to vapor being the "wetting" phase. As expected, for a given volume fraction ε_ℓ, there is a strong impact of the phases repartition on the effective properties. This emphasized the difficulties that one may encounter when dealing with a fully closed theory as discussed in Section 4. Indeed, when performing macro-scale calculations, one is faced with the problem of determining the most relevant repartition on the basis of some macro-scale selection criteria. An analysis about the meaning of each repartition for the stratified cell is carried out in [27] by returning to the pore-scale temperature fields through the representations (49)–(51) and by discarding the macroscopic temperature gradients. In this case, it is shown as first approximation that the s–ℓ–g configuration corresponds rather to condensation situations while the s–g–ℓ one corresponds rather to vaporization situations. From a practical point of view, this analysis suggests that both the volume fraction ε_ℓ and the sign of the difference between $\langle T_s \rangle^s$ and the saturation temperature would be possible candidates to play the role of a selection criterion. Although this analysis is quite limited owing to the simplifying assumptions and the simplicity of the stratified unit cell, it is instructive and it can serve as a starting point to develop useful *transition laws* for the effective coefficients. The interested reader is referred to [11] and [30] for some practical illustrations involving macro-scale calculations.

To complete the above discussion, we now turn back to the determination of the effective coefficients for more complex unit cells than those considered in this paper. As previously mentioned, the unit cell can be in principle as complex as needed to capture most of the features of a real system. For such more sophisticated unit cells, the route to obtain the effective coefficients is as follows:

(i) for a given periodic unit cell which defines the geometry for the solid phase, solve first the two-phase flow problem to provide the required velocity field and the interface topology,
(ii) then solve numerically the six closure problems and compute the effective coefficients.

Here, one must keep in mind that this route lies within the framework of a fully closed theory and as a result, the calculations are carried out for various arbitrary liquid volume fractions and macroscopic velocities or pressure gradients as well as phases repartition but without being interested in the historical evolution of the liquid–vapor interface. While the fully closed theory has its previously discussed limitations, it remains of a great practical interest and it can serve to assess the impact of several pore-scale parameters on the effective coefficients. Returning to the route (i)–(ii), the first step can be carried out by performing a direct numerical simulation of the two-phase flow over the periodic unit cell. This can be accomplished by means of some well known efficient methods for simulating small-scales interfacial phenomena such as front-tracking, volume-of-fluid or diffuse-interface methods. This methodology clearly illustrates the interest of the up-scaling approach since one can study the impact of several pore-scale characteristics on the basis of a detailed description of both the geometry and the pore-scale two-phase flow structure. Such developments are currently under way to generate numerical data for various pore-scale configurations and we refer the reader to [27] for some illustrations. From these calculations, our objective is to develop *numerical correlations* for the effective coefficients that can be used for macro-scale applications. While the approach is very attractive since it links the behavior of the effective coefficients with an accurate description of the pore-scale physics, it must be pointed out that there are some limitations regarding the complexity of the unit cells owing to the evident computational limitations. In practice, the use of a two-phase flow direct numerical simulation is tractable for unit cells containing a relatively small number of pores ranging typically from one to around ten pores. From a practical point of view, this may have important consequences regarding the behavior of the effective coefficients. Indeed, previous works in the case of contaminants transport in porous media [1,57] suggest that such unit cells may produce an extremely complex behavior (e.g. highly non-linear behavior versus the liquid volume fraction and the cell Péclet numbers, velocity orientation effects, etc.) while more complex, random, geometries involving thousands of pores may greatly simplify these complex features. It is beyond the scope of this paper to address this problem but several strategies can be develop to deal with very complicated geometries such as ensemble averaging of obtained results on simple geometries or as proposed by Ahmadi et al. [1] the use of network models. Both approaches, simple and complex geometries, open very interesting perspectives and call for further studies.

8. Numerical experiments for purely diffusive phase-change problems

The validity of the macro-scale three-equation model can be addressed according to two different ways, through laboratory experiments or through numerical "experiments". The former refers to comparisons with available experimental data while the latter uses direct pore-scale calculations as a reference solution. In both of

them, comparison is preferably performed in terms of averaged temperatures owing to the evident complexity associated with the experimental determination, or the direct estimation from micro-scale calculations, of the effective properties.

While comparisons with laboratory experiments represent obviously an important stage that cannot be overlooked to assess the quality and the contribution of the proposed macroscopic description, the analysis is made limited mainly because of the difficulties associated with the experimental measurements as pointed out in the introduction. A typical illustration of these difficulties lies in the flooding of a heat-generating porous bed which represents a problem of considerable interest in nuclear safety studies. Indeed, even though experimental results reveal large macro-scale temperature differences, these are rather difficult to determine from a quantitative point of view. As a result, available experimental data for this class of problems are often restricted to some overall quantities of interest at the scale of the sample such as the critical dryout heat flux or the steam flow rate at the top of the bed. Other difficulties mentioned in the previous section are encountered when dealing with full macro-scale calculations and comparisons with laboratory experiments for real systems. It is beyond the scope of this paper to deal with these difficulties and we refer the reader to Béchaud et al. [11] and Fichot et al. [30] for a detailed analysis and for practical applications using the proposed three-equation model.

On the other hand, numerical experiments consisting of pore-scale calculations used to determine averaged temperatures represent very good tests for the theory because pore-scale characteristics can be controlled precisely. To be more clear, numerical experiments provide the most direct test of the theory since the pore-scale equations are solved directly in the absence of some adjustable parameters.

Following the methodology outlined in Quintard et al. [54] in the framework of two-equation models, we focus here on purely diffusive processes with phase change and we perform comparisons between the theoretical predictions using the three-equation model, and the average of the direct solution of the pore-scale equations for both the stratified and the Chang's unit cell presented in appendix. It must be emphasized that the theoretical computations and the pore-scale ones are carried out in a completely independent manner. Therefore, such a comparison represents a strong test of the proposed model and allows us to investigate the impact of some of the simplifications that have been made at the closure level.

8.1. Solution of the macro-scale equations

Even though purely diffusive processes with phase change represent a very simplified case of what occurs in real systems, the macro-scale problem remains quite complicated in the sense that we must solve the three-equation model together with the macro-scale mass and momentum transport equations. In order to facilitate the numerical experiments and to focus on the thermal up-scaling problem, we assume the phase change does not involve significant changes in pressure and hence we impose the constraint of a constant pressure. In addition we require that there is a constant macroscopic density for both the vapor and the liquid phase so that $\rho_g = \rho_\ell = \rho$. Under these circumstances, the three-equation model supplemented by a governing equation for the liquid saturation $S = \varepsilon_\ell/\varepsilon$ is sufficient to describe the whole macroscopic behavior. The liquid saturation governing equation can be obtained from either the vapor continuity equation (18) or the liquid continuity equation (19) and reads

$$\varepsilon \frac{\partial S}{\partial t} = -\frac{\dot{m}}{\rho} \tag{70}$$

On the other hand, if we make the additional assumption that the system is infinite in all direction so that there is no gradient of the averaged temperatures, the three-equation model simplifies to

$$\begin{aligned}\varepsilon_g(\rho C_p)_g \frac{\partial \langle T_g\rangle^g}{\partial t} &= -\dot{m}C^*_{pg}(\langle T_g\rangle^g - T^{sat}) - (h^{g\ell}_{gi} + h^{gs}_{gi})(\langle T_g\rangle^g - T^{sat}) \\ &\quad - (h^{g\ell}_{si} + h^{gs}_{si})(\langle T_s\rangle^s - T^{sat})\end{aligned} \tag{71}$$

$$\varepsilon_\ell(\rho C_p)_\ell \frac{\partial \langle T_\ell\rangle^\ell}{\partial t} = \dot{m}C^*_{p\ell}(\langle T_\ell\rangle^\ell - T^{sat}) - h^{\ell g}_{\ell i}(\langle T_\ell\rangle^\ell - T^{sat}) \tag{72}$$

$$\begin{aligned}\varepsilon_s(\rho C_p)_s \frac{\partial \langle T_s\rangle^s}{\partial t} &= h^{gs}_{gi}(\langle T_g\rangle^g - T^{sat}) + h^{gs}_{si}(\langle T_s\rangle^s - T^{sat}) + \varepsilon_s\langle \varpi_s\rangle^s\end{aligned} \tag{73}$$

Here the quantities C^*_{pg} and $C^*_{p\ell}$ denote *fictitious heat capacities* calculated from the volumetric heat capacities $(\rho C_p)_g$ and $(\rho C_p)_\ell$ respectively, divided by the common density ρ. This definition allows us to maintain physical values of the thermal diffusivity for both the vapor and the liquid phase under the assumption of a constant density. Finally, neglecting the macroscopic temperature gradients, the phase change rate appearing in Eqs. (70)–(72) reduces to

$$\begin{aligned}\dot{m}\Delta h &= h^{\ell g}_{\ell i}(\langle T_\ell\rangle^\ell - T^{sat}) + h^{g\ell}_{gi}(\langle T_g\rangle^g - T^{sat}) \\ &\quad + h^{g\ell}_{si}(\langle T_s\rangle^s - T^{sat})\end{aligned} \tag{74}$$

In these equations, we will use the appropriate heat exchange coefficients obtained for the stratified and the Chang's unit cells. In writing Eqs. (71)–(74), it must be noted that some additional simplifications of the heat exchange coefficients arose because we have focussed on the

vapor-wetting pore-scale configuration denoted as s–g–ℓ in the appendix. This is due to the fact that the considered tests consist in evaporation processes and as indicated in Section 7, this corresponds to a vapor-wetting case.

8.2. Numerical solution of the pore-scale equations

In this section we describe briefly how we obtain the pore-scale temperature fields that will be averaged to produce the reference values for the numerical experiments. We recall here that under the previously listed assumptions the numerical experiments focus on pore-scale Stefan-like problems. At the pore-scale, the one-dimensional heat-diffusion moving boundary value problem is solved numerically using an enthalpy method. Hence, the micro-scale problem to be solved is formulated as

$$\frac{\partial \mathscr{H}(T)}{\partial t} = \nabla \cdot (k \nabla T) + \gamma_s \varpi_s, \quad \text{in } V \tag{75}$$

$$\mathbf{n} \cdot \nabla T = 0, \quad \text{at } \partial V \tag{76}$$

$$T(t=0) = T_0 \tag{77}$$

in which V is the volume of the unit cell and γ_s is the s-phase indicator function. In these equations, the volumetric enthalpy $\mathscr{H}$, the temperature and the conductivity are distributions defined in accordance with the thermal properties of the three phases. In Eq. (75), the $\mathscr{H}(T)$ function is defined as $\mathscr{H}(T) = (\rho C_p)_s T$ in the solid phase while the enthalpy–temperature relationship regularization proposed in [28] is used in the liquid and the vapor phases:

$$\mathscr{H}(T) = \begin{cases} \rho C^*_{p\ell} T + \frac{\rho \Delta h}{2} \exp\left(-\frac{|T - T^{\text{sat}}|}{\Delta T^-} \right), & T < T^{\text{sat}} \\ \rho C^*_{p\ell} T^{\text{sat}} + \rho \Delta h + \rho C^*_{pg} (T - T^{\text{sat}}) \\ \quad - \frac{\rho \Delta h}{2} \exp\left(-\frac{|T - T^{\text{sat}}|}{\Delta T^+} \right), & T \geqslant T^{\text{sat}} \end{cases} \tag{78}$$

where ΔT^- and ΔT^+ are the liquid–vapor front spreading parameters. Using a similar regularization for the conductivity distribution, the enthalpy equation is discretised by an implicit finite element method and is solved by a Newton's method. Because of the considered unit cells symmetry, direct computations have been performed on the half-cell $0 \leqslant y \leqslant H/2$ for the stratified unit cell and $0 \leqslant r \leqslant R$ for the Chang's unit cell. It is beyond the scope of this paper to describe the whole numerical method and we refer the interested reader to [27] for a detailed presentation. Here we will just note that the spreading parameters have been adjusted with grid refinements to achieve convergence results.

8.3. Comparison between theory and pore-scale simulations

Two numerical experiments consisting in a heating and a temperature relaxation problems were carried out for the unit cells shown in Figs. 10 and 12. The parameters for these experiments are listed in Table 1. Both the solid volume fraction ε_s and the solid phase characteristic length ℓ_s are the same for the two unit cells considered but it must be pointed out that the unit cells characteristic lengths are different because of $\ell_s = H\varepsilon_s$ for the stratified unit cell and $\ell_s = 2R\sqrt{\varepsilon_s}$ for the Chang's unit cell.

Table 1
Parameters for experiments with $T^{\text{sat}} = 373$ K and $\Delta h = 2.2 \times 10^6$ J kg^{-1}

Unit cells	ε_s	ℓ_s [m]	
	0.6	0.01	
Densities [kg m^{-3}]	ρ_g	ρ_ℓ	ρ_s
	1000	1000	7000
Volumetric heat capacities [J m^{-3} K^{-1}]	$(\rho C_p)_g$	$(\rho C_p)_\ell$	$(\rho C_p)_s$
	2×10^3	4.2×10^6	3.5×10^6
Thermal conductivities [W m^{-1} K^{-1}]	k_g	k_ℓ	k_s
	0.025	0.68	17

The first experiment looks at a heating problem starting with a saturated medium $S = 1$, local thermal equilibrium between the three phases, $\langle T_g \rangle^g = \langle T_\ell \rangle^\ell = \langle T_s \rangle^s = T^{\text{sat}}$, and volumetric heating in the solid phase $\langle \varpi_s \rangle^s = 10^7$ W m^{-3}. The second experiment looks at a temperature relaxation problem starting with an unsaturated medium without heating but with an initial thermal non-equilibrium such as $\langle T_\ell \rangle^\ell = T^{\text{sat}}$, $\langle T_g \rangle^g = \langle T_\ell \rangle^\ell + 30$ K and $\langle T_s \rangle^s = \langle T_\ell \rangle^\ell + 60$ K. Using a linear profile for the initialization of the pore-scale temperature field in the vapor phase, the corresponding saturation values for the stratified and the Chang's unit cells are $S = 0.9$ and $S \simeq 0.88$ respectively. Before looking at the results, it must be noticed that the "experimental" front position is obtained indirectly by reconstruction from the temperature field because of the use of an enthalpy method. The $\langle T_g \rangle^g$-experimental value is computed from both this front position and the temperature field. As a consequence, both the reference saturation and the reference $\langle T_g \rangle^g$ evolutions show some minor oscillatory behavior which is an inherent characteristic of the enthalpy method.

The comparison between the theoretical solutions $\langle T_g \rangle^g$ and $\langle T_s \rangle^s$ obtained from the three-equation model and the reference values obtained from the pore-scale direct solution are reported in Figs. 3 and 4 for the first experiment and in Figs. 5 and 6 for the second experiment. For both experiments, the average liquid temperature $\langle T_\ell \rangle^\ell$ remains constant during the process at a value $\langle T_\ell \rangle^\ell = T^{\text{sat}}$ and is not plotted. The theoretical prediction and reference saturation evolutions versus time are reported in Figs. 7 and 8 for the heating and the relaxation experiments respectively. These results show that theoretical values are in very good agreement with

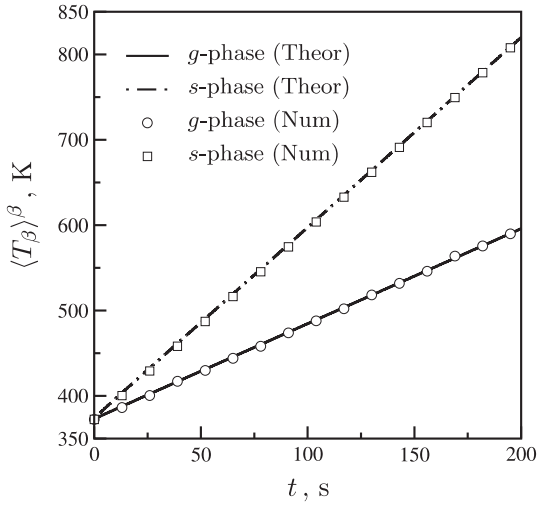

Fig. 3. Stratified unit cell: heating experiment (exp. 1).

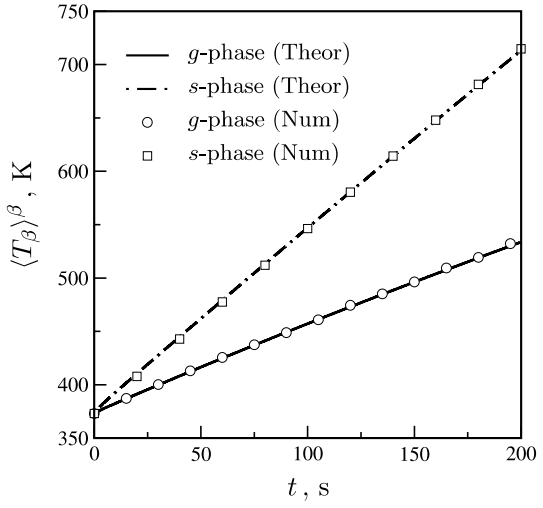

Fig. 4. Chang's unit cell: heating experiment (exp. 1).

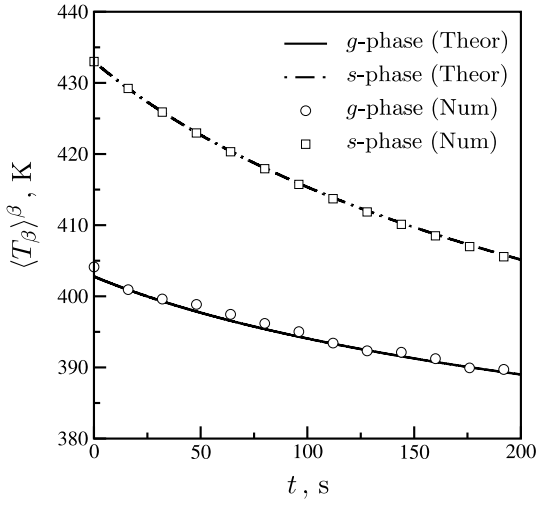

Fig. 5. Stratified unit cell: relaxation experiment (exp. 2).

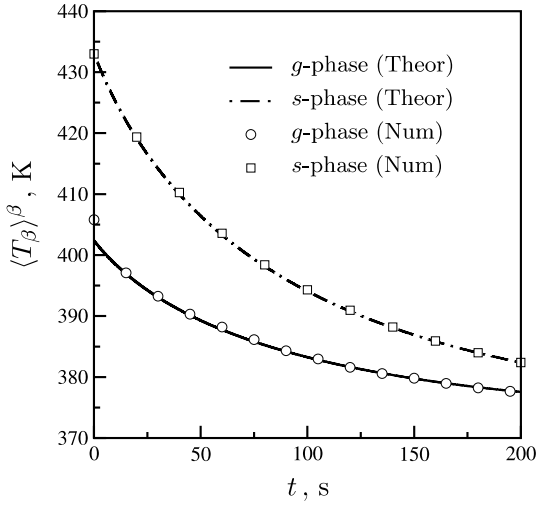

Fig. 6. Chang's unit cell: relaxation experiment (exp. 2).

"experimental" values despite the fact that both experiments are strongly unsteady and the thermal diffusivities are highly contrasted. Obviously, the parameters used for these experiments are not fully consistent with a liquid–vapor system because of our simplifying assumptions and as a result these experiments are mainly illustrative. Nevertheless, these simple tests allow us to illustrate the good behavior of the proposed approximate solution of the coupled micro-scale and macro-scale equations and the validity of the non-equilibrium model. These also confirm the practical interest of the three-equation model to deal with overheated porous structure reflooding problems where such large macro-scale temperature differences are expected (see for instance [49,72]). We must remind the reader that this is a partial validation obtained for purely diffusive processes. Work is under way to obtain direct numerical simulations with convection processes.

In obtaining these results, one should keep in mind that we have used the appropriate heat transfer coefficients obtained by *solving the closure problems*. At this point, one may ask the question whether other coefficients would also give a correct answer ? In order to clarify this point, we have repeated the heating experiment for the stratified unit cell by multiplying the coefficient $h_{\mathrm{gi}}^{\mathrm{gs}}$ by a factor three. The results are reported in

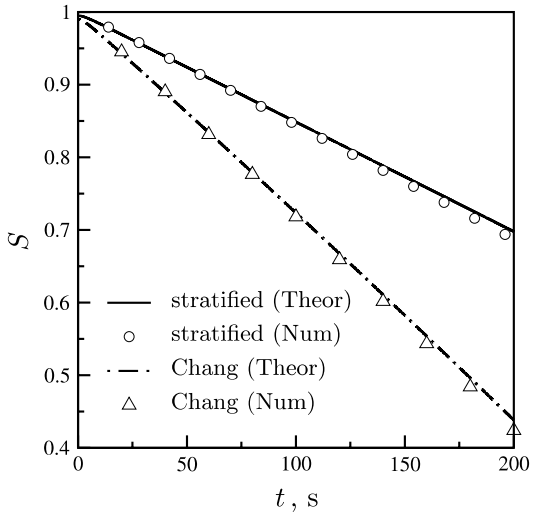

Fig. 7. Saturation evolution versus time for the heating experiment (exp. 1).

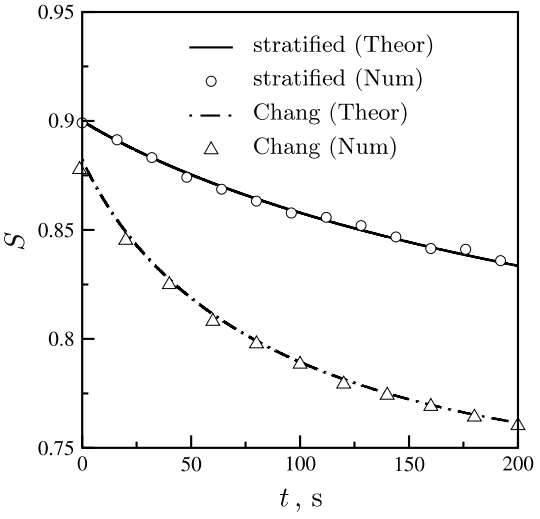

Fig. 8. Saturation evolution versus time for the relaxation experiment (exp. 2).

Fig. 9 in terms of the g-phase and s-phase macro-scale temperature evolutions versus time. Here again the average liquid temperature is not plotted because it remains equal to the saturation temperature during the process. The results show a significant difference when comparing to the original results obtained with the appropriate heat transfer coefficient. This clearly illustrates that the macro-scale behavior cannot be correctly captured with a priori estimates of the heat transfer coefficients and emphasizes the interest in using an up-scaling theory.

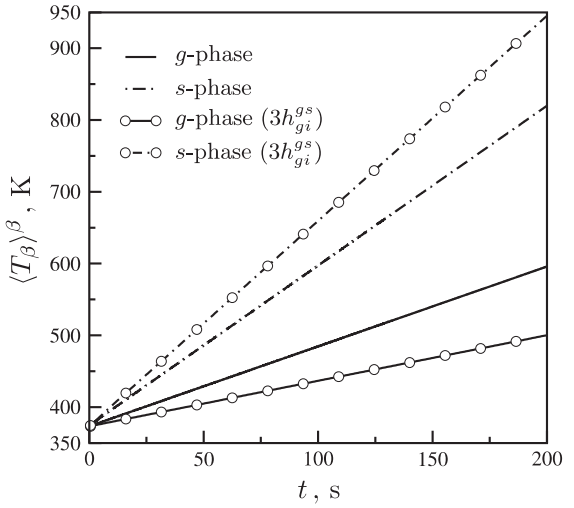

Fig. 9. Time evolution of the macro-scale temperatures from the three-equation model for the heating experiment on the stratified unit cell. Comparisons between the appropriate value for $h_{\mathrm{gi}}^{\mathrm{gs}}$ and the a priori estimate $3h_{\mathrm{gi}}^{\mathrm{gs}}$.

9. Conclusion

In this paper, the method of volume averaging has been used to derive a macroscopic model describing heat transfer processes for liquid–vapor flows with phase change in porous media. Under the classical quasi-steady and quasi-static assumptions at the closure level, the resulting macroscopic model is a three-equation model involving relevant non-equilibrium terms in which the saturation temperature appears explicitly. An attractive feature of the scaling-up theory lies in the derivation of a closed form of the evaporation rate at the macroscopic level depending on the macroscopic temperatures and the effective properties. The effective transport coefficients are related to the pore-scale physics through six closure problems that have to be solved for representative unit cells. These closure problems have been solved for simple unit cells to provide first estimates of the effective properties. For these unit cells and for purely diffusive processes, theoretical predictions of the three-equation model and numerical experiments are in very good agreement. This provides support for the assumptions and the simplifications that have been made at the closure level and illustrates the practical interest of the three-equation model.

Acknowledgements

Financial support from Institut de Radioprotection et de Sûreté Nucléaire (department DRS/SEMAR) is gratefully acknowledged.

Appendix A. Pore-scale closure problems

The pore-scale closure problems are obtained by introducing the representations (49)–(51) into the governing equations for the deviations (40)–(48), collecting all terms proportional to the six macroscopic source terms such as $(\langle T_\ell\rangle^\ell - T^{\mathrm{sat}})$, $\nabla\langle T_\mathrm{g}\rangle^\mathrm{g}$, etc., and setting the coefficients equal to zero. On the basis of the representations for the deviations, it must be emphasized that the three conditions $\langle\widetilde{T}_\mathrm{g}\rangle^\mathrm{g} = \langle\widetilde{T}_\ell\rangle^\ell = \langle\widetilde{T}_\mathrm{s}\rangle^\mathrm{s} = 0$ require that the intrinsic phase average of the closure variables are equal to zero, this provides additional relations for the closure problems.

The first three closure problems are the boundary value problems associated with the mapping variables for $(\langle T_\ell\rangle^\ell - T^{\mathrm{sat}})$, $(\langle T_\mathrm{g}\rangle^\mathrm{g} - T^{\mathrm{sat}})$ and $(\langle T_\mathrm{s}\rangle^\mathrm{s} - T^{\mathrm{sat}})$, these problems are listed below.

Problem I. $(\langle T_\ell\rangle^\ell - T^{\mathrm{sat}})$ mapping

$$(\rho C_p)_\mathrm{g}\mathbf{v}_\mathrm{g}\cdot\nabla s^\mathrm{g}_{\ell\mathrm{i}} = k_\mathrm{g}\nabla^2 s^\mathrm{g}_{\ell\mathrm{i}} - \varepsilon_\mathrm{g}^{-1}(h^{\mathrm{g}\ell}_{\ell\mathrm{i}} + h^{\mathrm{gs}}_{\ell\mathrm{i}}), \quad \text{in the g-phase} \tag{A.1}$$

$$s^\mathrm{g}_{\ell\mathrm{i}} = 0, \quad s^\ell_{\ell\mathrm{i}} = 1, \quad \text{at } A_{\ell\mathrm{g}} \tag{A.2}$$

$$\mathbf{n}_{\mathrm{gs}}\cdot k_\mathrm{s}\nabla s^\mathrm{s}_{\ell\mathrm{i}} = \mathbf{n}_{\mathrm{gs}}\cdot k_\mathrm{g}\nabla s^\mathrm{g}_{\ell\mathrm{i}}, \quad s^\mathrm{g}_{\ell\mathrm{i}} = s^\mathrm{s}_{\ell\mathrm{i}}, \quad \text{at } A_{\mathrm{gs}} \tag{A.3}$$

$$(\rho C_p)_\ell\mathbf{v}_\ell\cdot\nabla s^\ell_{\ell\mathrm{i}} = k_\ell\nabla^2 s^\ell_{\ell\mathrm{i}} - \varepsilon_\ell^{-1}(h^{\ell\mathrm{g}}_{\ell\mathrm{i}} + h^{\ell\mathrm{s}}_{\ell\mathrm{i}}), \quad \text{in the } \ell\text{-phase} \tag{A.4}$$

$$\mathbf{n}_{\ell\mathrm{s}}\cdot k_\ell\nabla s^\ell_{\ell\mathrm{i}} = \mathbf{n}_{\ell\mathrm{s}}\cdot k_\mathrm{s}\nabla s^\mathrm{s}_{\ell\mathrm{i}}, \quad s^\ell_{\ell\mathrm{i}} = s^\mathrm{s}_{\ell\mathrm{i}} + 1, \quad \text{at } A_{\ell\mathrm{s}} \tag{A.5}$$

$$0 = k_\mathrm{s}\nabla^2 s^\mathrm{s}_{\ell\mathrm{i}} - \varepsilon_\mathrm{s}^{-1}(h^{\mathrm{sg}}_{\ell\mathrm{i}} + h^{\mathrm{s}\ell}_{\ell\mathrm{i}}), \quad \text{in the s-phase} \tag{A.6}$$

$$\text{Periodicity:}\quad s^\ell_{\ell\mathrm{i}}(\mathbf{r}+l_i) = s^\ell_{\ell\mathrm{i}}(\mathbf{r}), \quad s^\mathrm{g}_{\ell\mathrm{i}}(\mathbf{r}+l_i) = s^\mathrm{g}_{\ell\mathrm{i}}(\mathbf{r}), \quad s^\mathrm{s}_{\ell\mathrm{i}}(\mathbf{r}+l_i) = s^\mathrm{s}_{\ell\mathrm{i}}(\mathbf{r}), \quad i=1,2,3 \tag{A.7}$$

$$\text{Average:}\quad \langle s^\ell_{\ell\mathrm{i}}\rangle^\ell = 0, \quad \langle s^\mathrm{g}_{\ell\mathrm{i}}\rangle^\mathrm{g} = 0, \quad \langle s^\mathrm{s}_{\ell\mathrm{i}}\rangle^\mathrm{s} = 0 \tag{A.8}$$

We have adopted the following notations

$$h^{\mathrm{g}\ell}_{\ell\mathrm{i}} = \frac{k_\mathrm{g}}{V}\int_{A_{\mathrm{g}\ell}}\mathbf{n}_{\mathrm{g}\ell}\cdot\nabla s^\mathrm{g}_{\ell\mathrm{i}}\,\mathrm{d}A, \quad h^{\mathrm{gs}}_{\ell\mathrm{i}} = \frac{k_\mathrm{g}}{V}\int_{A_{\mathrm{gs}}}\mathbf{n}_{\mathrm{gs}}\cdot\nabla s^\mathrm{g}_{\ell\mathrm{i}}\,\mathrm{d}A \tag{A.9}$$

$$h^{\ell\mathrm{g}}_{\ell\mathrm{i}} = \frac{k_\ell}{V}\int_{A_{\ell\mathrm{g}}}\mathbf{n}_{\ell\mathrm{g}}\cdot\nabla s^\ell_{\ell\mathrm{i}}\,\mathrm{d}A, \quad h^{\ell\mathrm{s}}_{\ell\mathrm{i}} = \frac{k_\ell}{V}\int_{A_{\ell\mathrm{s}}}\mathbf{n}_{\ell\mathrm{s}}\cdot\nabla s^\ell_{\ell\mathrm{i}}\,\mathrm{d}A \tag{A.10}$$

$$h^{\mathrm{sg}}_{\ell\mathrm{i}} = \frac{k_\mathrm{s}}{V}\int_{A_{\mathrm{sg}}}\mathbf{n}_{\mathrm{sg}}\cdot\nabla s^\mathrm{s}_{\ell\mathrm{i}}\,\mathrm{d}A = -h^{\mathrm{gs}}_{\ell\mathrm{i}}, \quad h^{\mathrm{s}\ell}_{\ell\mathrm{i}} = \frac{k_\mathrm{s}}{V}\int_{A_{\mathrm{s}\ell}}\mathbf{n}_{\mathrm{s}\ell}\cdot\nabla s^\mathrm{s}_{\ell\mathrm{i}}\,\mathrm{d}A = -h^{\ell\mathrm{s}}_{\ell\mathrm{i}} \tag{A.11}$$

Problem II. $(\langle T_\mathrm{g}\rangle^\mathrm{g} - T^{\mathrm{sat}})$ mapping

$$(\rho C_p)_\mathrm{g}\mathbf{v}_\mathrm{g}\cdot\nabla s^\mathrm{g}_{\mathrm{gi}} = k_\mathrm{g}\nabla^2 s^\mathrm{g}_{\mathrm{gi}} - \varepsilon_\mathrm{g}^{-1}(h^{\mathrm{g}\ell}_{\mathrm{gi}} + h^{\mathrm{gs}}_{\mathrm{gi}}), \quad \text{in the g-phase} \tag{A.12}$$

$$s^\mathrm{g}_{\mathrm{gi}} = 1, \quad s^\ell_{\mathrm{gi}} = 0, \quad \text{at } A_{\ell\mathrm{g}} \tag{A.13}$$

$$\mathbf{n}_{\mathrm{gs}}\cdot k_\mathrm{s}\nabla s^\mathrm{s}_{\mathrm{gi}} = \mathbf{n}_{\mathrm{gs}}\cdot k_\mathrm{g}\nabla s^\mathrm{g}_{\mathrm{gi}}, \quad s^\mathrm{g}_{\mathrm{gi}} = s^\mathrm{s}_{\mathrm{gi}} + 1, \quad \text{at } A_{\mathrm{gs}} \tag{A.14}$$

$$(\rho C_p)_\ell\mathbf{v}_\ell\cdot\nabla s^\ell_{\mathrm{gi}} = k_\ell\nabla^2 s^\ell_{\mathrm{gi}} - \varepsilon_\ell^{-1}(h^{\ell\mathrm{g}}_{\mathrm{gi}} + h^{\ell\mathrm{s}}_{\mathrm{gi}}), \quad \text{in the } \ell\text{-phase} \tag{A.15}$$

$$\mathbf{n}_{\ell\mathrm{s}}\cdot k_\ell\nabla s^\ell_{\mathrm{gi}} = \mathbf{n}_{\ell\mathrm{s}}\cdot k_\mathrm{s}\nabla s^\mathrm{s}_{\mathrm{gi}}, \quad s^\ell_{\mathrm{gi}} = s^\mathrm{s}_{\mathrm{gi}}, \quad \text{at } A_{\ell\mathrm{s}} \tag{A.16}$$

$$0 = k_\mathrm{s}\nabla^2 s^\mathrm{s}_{\mathrm{gi}} - \varepsilon_\mathrm{s}^{-1}(h^{\mathrm{sg}}_{\mathrm{gi}} + h^{\mathrm{s}\ell}_{\mathrm{gi}}), \quad \text{in the s-phase} \tag{A.17}$$

$$\text{Periodicity:}\quad s^\ell_{\mathrm{gi}}(\mathbf{r}+l_i) = s^\ell_{\mathrm{gi}}(\mathbf{r}), \quad s^\mathrm{g}_{\mathrm{gi}}(\mathbf{r}+l_i) = s^\mathrm{g}_{\mathrm{gi}}(\mathbf{r}), \quad s^\mathrm{s}_{\mathrm{gi}}(\mathbf{r}+l_i) = s^\mathrm{s}_{\ell\mathrm{i}}(\mathbf{r}), \quad i=1,2,3 \tag{A.18}$$

$$\text{Average:}\quad \langle s^\ell_{\mathrm{gi}}\rangle^\ell = 0, \quad \langle s^\mathrm{g}_{\mathrm{gi}}\rangle^\mathrm{g} = 0, \quad \langle s^\mathrm{s}_{\mathrm{gi}}\rangle^\mathrm{s} = 0 \tag{A.19}$$

We have adopted the following notations

$$h^{\mathrm{g}\ell}_{\mathrm{gi}} = \frac{k_\mathrm{g}}{V}\int_{A_{\mathrm{g}\ell}}\mathbf{n}_{\mathrm{g}\ell}\cdot\nabla s^\mathrm{g}_{\mathrm{gi}}\,\mathrm{d}A, \quad h^{\mathrm{gs}}_{\mathrm{gi}} = \frac{k_\mathrm{g}}{V}\int_{A_{\mathrm{gs}}}\mathbf{n}_{\mathrm{gs}}\cdot\nabla s^\mathrm{g}_{\mathrm{gi}}\,\mathrm{d}A \tag{A.20}$$

$$h^{\ell\mathrm{g}}_{\mathrm{gi}} = \frac{k_\ell}{V}\int_{A_{\ell\mathrm{g}}}\mathbf{n}_{\ell\mathrm{g}}\cdot\nabla s^\ell_{\mathrm{gi}}\,\mathrm{d}A, \quad h^{\ell\mathrm{s}}_{\mathrm{gi}} = \frac{k_\ell}{V}\int_{A_{\ell\mathrm{s}}}\mathbf{n}_{\ell\mathrm{s}}\cdot\nabla s^\ell_{\mathrm{gi}}\,\mathrm{d}A \tag{A.21}$$

$$h^{\mathrm{sg}}_{\mathrm{gi}} = \frac{k_\mathrm{s}}{V}\int_{A_{\mathrm{sg}}}\mathbf{n}_{\mathrm{sg}}\cdot\nabla s^\mathrm{s}_{\mathrm{gi}}\,\mathrm{d}A = -h^{\mathrm{gs}}_{\mathrm{gi}}, \quad h^{\mathrm{s}\ell}_{\mathrm{gi}} = \frac{k_\mathrm{s}}{V}\int_{A_{\mathrm{s}\ell}}\mathbf{n}_{\mathrm{s}\ell}\cdot\nabla s^\mathrm{s}_{\mathrm{gi}}\,\mathrm{d}A = -h^{\ell\mathrm{s}}_{\mathrm{gi}} \tag{A.22}$$

Problem III. $(\langle T_\mathrm{s}\rangle^\mathrm{s} - T^{\mathrm{sat}})$ mapping

$$(\rho C_p)_\mathrm{g}\mathbf{v}_\mathrm{g}\cdot\nabla s^\mathrm{g}_{\mathrm{si}} = k_\mathrm{g}\nabla^2 s^\mathrm{g}_{\mathrm{si}} - \varepsilon_\mathrm{g}^{-1}(h^{\mathrm{g}\ell}_{\mathrm{si}} + h^{\mathrm{gs}}_{\mathrm{si}}), \quad \text{in the g-phase} \tag{A.23}$$

$$s^\mathrm{g}_{\mathrm{si}} = 0, \quad s^\ell_{\mathrm{si}} = 0, \quad \text{at } A_{\ell\mathrm{g}} \tag{A.24}$$

$$\mathbf{n}_{\mathrm{gs}}\cdot k_\mathrm{s}\nabla s^\mathrm{s}_{\mathrm{si}} = \mathbf{n}_{\mathrm{gs}}\cdot k_\mathrm{g}\nabla s^\mathrm{g}_{\mathrm{si}}, \quad s^\mathrm{g}_{\mathrm{si}} = s^\mathrm{s}_{\mathrm{si}} - 1, \quad \text{at } A_{\mathrm{gs}} \tag{A.25}$$

$$(\rho C_p)_\ell\mathbf{v}_\ell\cdot\nabla s^\ell_{\mathrm{si}} = k_\ell\nabla^2 s^\ell_{\mathrm{si}} - \varepsilon_\ell^{-1}(h^{\ell\mathrm{g}}_{\mathrm{si}} + h^{\ell\mathrm{s}}_{\mathrm{si}}), \quad \text{in the } \ell\text{-phase} \tag{A.26}$$

$$\mathbf{n}_{\ell\mathrm{s}}\cdot k_\ell\nabla s^\ell_{\mathrm{si}} = \mathbf{n}_{\ell\mathrm{s}}\cdot k_\mathrm{s}\nabla s^\mathrm{s}_{\mathrm{si}}, \quad s^\ell_{\mathrm{si}} = s^\mathrm{s}_{\mathrm{si}} - 1, \quad \text{at } A_{\ell\mathrm{s}} \tag{A.27}$$

$$0 = k_\mathrm{s}\nabla^2 s^\mathrm{s}_{\mathrm{si}} - \varepsilon_\mathrm{s}^{-1}(h^{\mathrm{sg}}_{\mathrm{si}} + h^{\mathrm{s}\ell}_{\mathrm{si}}), \quad \text{in the s-phase} \tag{A.28}$$

$$\text{Periodicity:}\quad s^\ell_{\mathrm{si}}(\mathbf{r}+l_i) = s^\ell_{\mathrm{si}}(\mathbf{r}), \quad s^\mathrm{g}_{\mathrm{si}}(\mathbf{r}+l_i) = s^\mathrm{g}_{\mathrm{si}}(\mathbf{r}), \quad s^\mathrm{s}_{\mathrm{si}}(\mathbf{r}+l_i) = s^\mathrm{s}_{\mathrm{si}}(\mathbf{r}), \quad i=1,2,3 \tag{A.29}$$

$$\text{Average:}\quad \langle s^\ell_{\mathrm{si}}\rangle^\ell = 0, \quad \langle s^\mathrm{g}_{\mathrm{si}}\rangle^\mathrm{g} = 0, \quad \langle s^\mathrm{s}_{\mathrm{si}}\rangle^\mathrm{s} = 0 \tag{A.30}$$

We have adopted the following notations

$$h^{\mathrm{g}\ell}_{\mathrm{si}} = \frac{k_\mathrm{g}}{V}\int_{A_{\mathrm{g}\ell}}\mathbf{n}_{\mathrm{g}\ell}\cdot\nabla s^\mathrm{g}_{\mathrm{si}}\,\mathrm{d}A, \quad h^{\mathrm{gs}}_{\mathrm{si}} = \frac{k_\mathrm{g}}{V}\int_{A_{\mathrm{gs}}}\mathbf{n}_{\mathrm{gs}}\cdot\nabla s^\mathrm{g}_{\mathrm{si}}\,\mathrm{d}A \tag{A.31}$$

$$h_{\mathrm{si}}^{\ell\mathrm{g}} = \frac{k_\ell}{V}\int_{A_{\ell\mathrm{g}}} \mathbf{n}_{\ell\mathrm{g}}\cdot\nabla s_{\mathrm{si}}^{\ell}\,\mathrm{d}A, \quad h_{\mathrm{si}}^{\ell\mathrm{s}} = \frac{k_\ell}{V}\int_{A_{\ell\mathrm{s}}} \mathbf{n}_{\ell\mathrm{s}}\cdot\nabla s_{\mathrm{si}}^{\ell}\,\mathrm{d}A \tag{A.32}$$

$$h_{\mathrm{si}}^{\mathrm{sg}} = \frac{k_\mathrm{s}}{V}\int_{A_{\mathrm{sg}}} \mathbf{n}_{\mathrm{sg}}\cdot\nabla s_{\mathrm{si}}^{\mathrm{s}}\,\mathrm{d}A = -h_{\mathrm{si}}^{\mathrm{gs}},$$
$$h_{\mathrm{si}}^{\mathrm{s}\ell} = \frac{k_\mathrm{s}}{V}\int_{A_{\mathrm{s}\ell}} \mathbf{n}_{\mathrm{s}\ell}\cdot\nabla s_{\mathrm{si}}^{\mathrm{s}}\,\mathrm{d}A = -h_{\mathrm{si}}^{\ell\mathrm{s}} \tag{A.33}$$

The closure problems IV, V, VI are the boundary value problems associated with the mapping variables for $\nabla\langle T_\mathrm{g}\rangle^{\mathrm{g}}$, $\nabla\langle T_\ell\rangle^{\ell}$ and $\nabla\langle T_\mathrm{s}\rangle^{\mathrm{s}}$, these problems are listed below.

Problem IV. $\nabla\langle T_\mathrm{g}\rangle^{\mathrm{g}}$ mapping

$$(\rho C_p)_\mathrm{g}\mathbf{v}_\mathrm{g}\cdot\nabla\mathbf{b}_{\mathrm{gg}} + (\rho C_p)_\mathrm{g}\widetilde{\mathbf{v}}_\mathrm{g} = k_\mathrm{g}\nabla^2\mathbf{b}_{\mathrm{gg}} - \varepsilon_\mathrm{g}^{-1}(\mathbf{c}_{\mathrm{gg}}^{\mathrm{g}\ell} + \mathbf{c}_{\mathrm{gg}}^{\mathrm{gs}}), \quad \text{in the g-phase} \tag{A.34}$$

$$\mathbf{b}_{\mathrm{gg}} = 0, \quad \mathbf{b}_{\ell\mathrm{g}} = 0, \quad \text{at } A_{\ell\mathrm{g}} \tag{A.35}$$

$$\mathbf{n}_{\mathrm{gs}}\cdot k_\mathrm{s}\nabla\mathbf{b}_{\mathrm{sg}} = \mathbf{n}_{\mathrm{gs}}\cdot k_\mathrm{g}\nabla\mathbf{b}_{\mathrm{gg}} + \mathbf{n}_{\mathrm{gs}}k_\mathrm{g}, \quad \mathbf{b}_{\mathrm{gg}} = \mathbf{b}_{\mathrm{sg}}, \quad \text{at } A_{\mathrm{gs}} \tag{A.36}$$

$$(\rho C_p)_\ell\mathbf{v}_\ell\cdot\nabla\mathbf{b}_{\ell\mathrm{g}} = k_\ell\nabla^2\mathbf{b}_{\ell\mathrm{g}} - \varepsilon_\ell^{-1}(\mathbf{c}_{\ell\mathrm{g}}^{\ell\mathrm{g}} + \mathbf{c}_{\ell\mathrm{g}}^{\ell\mathrm{s}}), \quad \text{in the } \ell\text{-phase} \tag{A.37}$$

$$\mathbf{n}_{\ell\mathrm{s}}\cdot k_\ell\nabla\mathbf{b}_{\ell\mathrm{g}} = \mathbf{n}_{\ell\mathrm{s}}\cdot k_\mathrm{s}\nabla\mathbf{b}_{\mathrm{sg}}, \quad \mathbf{b}_{\ell\mathrm{g}} = \mathbf{b}_{\mathrm{sg}}, \quad \text{at } A_{\ell\mathrm{s}} \tag{A.38}$$

$$0 = k_\mathrm{s}\nabla^2\mathbf{b}_{\mathrm{sg}} - \varepsilon_\mathrm{s}^{-1}(\mathbf{c}_{\mathrm{sg}}^{\mathrm{s}\ell} + \mathbf{c}_{\mathrm{sg}}^{\mathrm{sg}}), \quad \text{in the s-phase} \tag{A.39}$$

$$\text{Periodicity:} \quad \mathbf{b}_{\ell\mathrm{g}}(\mathbf{r}+l_i) = \mathbf{b}_{\ell\mathrm{g}}(\mathbf{r}), \quad \mathbf{b}_{\mathrm{gg}}(\mathbf{r}+l_i) = \mathbf{b}_{\mathrm{gg}}(\mathbf{r}), \quad \mathbf{b}_{\mathrm{sg}}(\mathbf{r}+l_i) = \mathbf{b}_{\mathrm{sg}}(\mathbf{r}), \quad i = 1,2,3 \tag{A.40}$$

$$\text{Average:} \quad \langle\mathbf{b}_{\ell\mathrm{g}}\rangle^{\ell} = 0, \quad \langle\mathbf{b}_{\mathrm{gg}}\rangle^{\mathrm{g}} = 0, \quad \langle\mathbf{b}_{\mathrm{sg}}\rangle^{\mathrm{s}} = 0 \tag{A.41}$$

We have adopted the following notations

$$\mathbf{c}_{\mathrm{gg}}^{\mathrm{g}\ell} = \frac{k_\mathrm{g}}{V}\int_{A_{\mathrm{g}\ell}} \mathbf{n}_{\mathrm{g}\ell}\cdot\nabla\mathbf{b}_{\mathrm{gg}}\,\mathrm{d}A,$$
$$\mathbf{c}_{\mathrm{gg}}^{\mathrm{gs}} = \frac{k_\mathrm{g}}{V}\int_{A_{\mathrm{gs}}} \mathbf{n}_{\mathrm{gs}}\cdot\nabla\mathbf{b}_{\mathrm{gg}}\,\mathrm{d}A = -\mathbf{c}_{\mathrm{sg}}^{\mathrm{sg}} - \frac{k_\mathrm{g}}{V}\int_{A_{\mathrm{gs}}} \mathbf{n}_{\mathrm{gs}}\,\mathrm{d}A \tag{A.42}$$

$$\mathbf{c}_{\ell\mathrm{g}}^{\ell\mathrm{g}} = \frac{k_\ell}{V}\int_{A_{\ell\mathrm{g}}} \mathbf{n}_{\ell\mathrm{g}}\cdot\nabla\mathbf{b}_{\ell\mathrm{g}}\,\mathrm{d}A,$$
$$\mathbf{c}_{\ell\mathrm{g}}^{\ell\mathrm{s}} = \frac{k_\ell}{V}\int_{A_{\ell\mathrm{s}}} \mathbf{n}_{\ell\mathrm{s}}\cdot\nabla\mathbf{b}_{\ell\mathrm{g}}\,\mathrm{d}A = -\mathbf{c}_{\mathrm{sg}}^{\mathrm{s}\ell} \tag{A.43}$$

$$\mathbf{c}_{\mathrm{sg}}^{\mathrm{s}\ell} = \frac{k_\mathrm{s}}{V}\int_{A_{\mathrm{s}\ell}} \mathbf{n}_{\mathrm{s}\ell}\cdot\nabla\mathbf{b}_{\mathrm{sg}}\,\mathrm{d}A, \quad \mathbf{c}_{\mathrm{sg}}^{\mathrm{sg}} = \frac{k_\mathrm{s}}{V}\int_{A_{\mathrm{sg}}} \mathbf{n}_{\mathrm{sg}}\cdot\nabla\mathbf{b}_{\mathrm{sg}}\,\mathrm{d}A \tag{A.44}$$

Problem V. $\nabla\langle T_\ell\rangle^{\ell}$ mapping

$$(\rho C_p)_\mathrm{g}\mathbf{v}_\mathrm{g}\cdot\nabla\mathbf{b}_{\mathrm{g}\ell} = k_\mathrm{g}\nabla^2\mathbf{b}_{\mathrm{g}\ell} - \varepsilon_\mathrm{g}^{-1}(\mathbf{c}_{\mathrm{g}\ell}^{\mathrm{g}\ell} + \mathbf{c}_{\mathrm{g}\ell}^{\mathrm{gs}}), \quad \text{in the g-phase} \tag{A.45}$$

$$\mathbf{b}_{\mathrm{g}\ell} = 0, \quad \mathbf{b}_{\ell\ell} = 0, \quad \text{at } A_{\ell\mathrm{g}} \tag{A.46}$$

$$\mathbf{n}_{\mathrm{gs}}\cdot k_\mathrm{s}\nabla\mathbf{b}_{\mathrm{s}\ell} = \mathbf{n}_{\mathrm{gs}}\cdot k_\mathrm{g}\nabla\mathbf{b}_{\mathrm{g}\ell}, \quad \mathbf{b}_{\mathrm{g}\ell} = \mathbf{b}_{\mathrm{s}\ell}, \quad \text{at } A_{\mathrm{gs}} \tag{A.47}$$

$$(\rho C_p)_\ell\mathbf{v}_\ell\cdot\nabla\mathbf{b}_{\ell\ell} + (\rho C_p)_\ell\widetilde{\mathbf{v}}_\ell = k_\ell\nabla^2\mathbf{b}_{\ell\ell} - \varepsilon_\ell^{-1}(\mathbf{c}_{\ell\ell}^{\ell\mathrm{g}} + \mathbf{c}_{\ell\ell}^{\ell\mathrm{s}}), \quad \text{in the } \ell\text{-phase} \tag{A.48}$$

$$\mathbf{n}_{\ell\mathrm{s}}\cdot k_\ell\nabla\mathbf{b}_{\ell\ell} = \mathbf{n}_{\ell\mathrm{s}}\cdot k_\mathrm{s}\nabla\mathbf{b}_{\mathrm{s}\ell} - \mathbf{n}_{\ell\mathrm{s}}k_\ell, \quad \mathbf{b}_{\ell\ell} = \mathbf{b}_{\mathrm{s}\ell}, \quad \text{at } A_{\ell\mathrm{s}} \tag{A.49}$$

$$0 = k_\mathrm{s}\nabla^2\mathbf{b}_{\mathrm{s}\ell} - \varepsilon_\mathrm{s}^{-1}(\mathbf{c}_{\mathrm{s}\ell}^{\mathrm{s}\ell} + \mathbf{c}_{\mathrm{s}\ell}^{\mathrm{sg}}), \quad \text{in the s-phase} \tag{A.50}$$

$$\text{Periodicity:} \quad \mathbf{b}_{\ell\ell}(\mathbf{r}+l_i) = \mathbf{b}_{\ell\ell}(\mathbf{r}), \quad \mathbf{b}_{\mathrm{g}\ell}(\mathbf{r}+l_i) = \mathbf{b}_{\mathrm{g}\ell}(\mathbf{r}), \quad \mathbf{b}_{\mathrm{s}\ell}(\mathbf{r}+l_i) = \mathbf{b}_{\mathrm{s}\ell}(\mathbf{r}), \quad i = 1,2,3 \tag{A.51}$$

$$\text{Average:} \quad \langle\mathbf{b}_{\ell\ell}\rangle^{\ell} = 0, \quad \langle\mathbf{b}_{\mathrm{g}\ell}\rangle^{\mathrm{g}} = 0, \quad \langle\mathbf{b}_{\mathrm{s}\ell}\rangle^{\mathrm{s}} = 0 \tag{A.52}$$

We have adopted the following notations

$$\mathbf{c}_{\mathrm{g}\ell}^{\mathrm{g}\ell} = \frac{k_\mathrm{g}}{V}\int_{A_{\mathrm{g}\ell}} \mathbf{n}_{\mathrm{g}\ell}\cdot\nabla\mathbf{b}_{\mathrm{g}\ell}\,\mathrm{d}A,$$
$$\mathbf{c}_{\mathrm{g}\ell}^{\mathrm{gs}} = \frac{k_\mathrm{g}}{V}\int_{A_{\mathrm{gs}}} \mathbf{n}_{\mathrm{gs}}\cdot\nabla\mathbf{b}_{\mathrm{g}\ell}\,\mathrm{d}A = -\mathbf{c}_{\mathrm{s}\ell}^{\mathrm{sg}} \tag{A.53}$$

$$\mathbf{c}_{\ell\ell}^{\ell\mathrm{g}} = \frac{k_\ell}{V}\int_{A_{\ell\mathrm{g}}} \mathbf{n}_{\ell\mathrm{g}}\cdot\nabla\mathbf{b}_{\ell\ell}\,\mathrm{d}A,$$
$$\mathbf{c}_{\ell\ell}^{\ell\mathrm{s}} = \frac{k_\ell}{V}\int_{A_{\ell\mathrm{s}}} \mathbf{n}_{\ell\mathrm{s}}\cdot\nabla\mathbf{b}_{\ell\ell}\,\mathrm{d}A = -\mathbf{c}_{\mathrm{s}\ell}^{\mathrm{s}\ell} - \frac{k_\ell}{V}\int_{A_{\ell\mathrm{s}}} \mathbf{n}_{\ell\mathrm{s}}\,\mathrm{d}A \tag{A.54}$$

$$\mathbf{c}_{\mathrm{s}\ell}^{\mathrm{s}\ell} = \frac{k_\mathrm{s}}{V}\int_{A_{\mathrm{s}\ell}} \mathbf{n}_{\mathrm{s}\ell}\cdot\nabla\mathbf{b}_{\mathrm{s}\ell}\,\mathrm{d}A, \quad \mathbf{c}_{\mathrm{s}\ell}^{\mathrm{sg}} = \frac{k_\mathrm{s}}{V}\int_{A_{\mathrm{sg}}} \mathbf{n}_{\mathrm{sg}}\cdot\nabla\mathbf{b}_{\mathrm{s}\ell}\,\mathrm{d}A \tag{A.55}$$

Problem VI. $\nabla\langle T_\mathrm{s}\rangle^{\mathrm{s}}$ mapping

$$(\rho C_p)_\mathrm{g}\mathbf{v}_\mathrm{g}\cdot\nabla\mathbf{b}_{\mathrm{gs}} = k_\mathrm{g}\nabla^2\mathbf{b}_{\mathrm{gs}} - \varepsilon_\mathrm{g}^{-1}(\mathbf{c}_{\mathrm{gs}}^{\mathrm{g}\ell} + \mathbf{c}_{\mathrm{gs}}^{\mathrm{gs}}), \quad \text{in the g-phase} \tag{A.56}$$

$$\mathbf{b}_{\mathrm{gs}} = 0, \quad \mathbf{b}_{\ell\mathrm{s}} = 0, \quad \text{at } A_{\ell\mathrm{g}} \tag{A.57}$$

$$\mathbf{n}_{\mathrm{gs}}\cdot k_\mathrm{s}\nabla\mathbf{b}_{\mathrm{ss}} = \mathbf{n}_{\mathrm{gs}}\cdot k_\mathrm{g}\nabla\mathbf{b}_{\mathrm{gs}} - \mathbf{n}_{\mathrm{gs}}k_\mathrm{s}, \quad \mathbf{b}_{\mathrm{gs}} = \mathbf{b}_{\mathrm{ss}}, \quad \text{at } A_{\mathrm{gs}} \tag{A.58}$$

$$(\rho C_p)_\ell\mathbf{v}_\ell\cdot\nabla\mathbf{b}_{\ell\mathrm{s}} = k_\ell\nabla^2\mathbf{b}_{\ell\mathrm{s}} - \varepsilon_\ell^{-1}(\mathbf{c}_{\ell\mathrm{s}}^{\ell\mathrm{g}} + \mathbf{c}_{\ell\mathrm{s}}^{\ell\mathrm{s}}), \quad \text{in the } \ell\text{-phase} \tag{A.59}$$

$$\mathbf{n}_{\ell\mathrm{s}}\cdot k_\ell\nabla\mathbf{b}_{\ell\mathrm{s}} = \mathbf{n}_{\ell\mathrm{s}}\cdot k_\mathrm{s}\nabla\mathbf{b}_{\mathrm{ss}} + \mathbf{n}_{\ell\mathrm{s}}k_\mathrm{s}, \quad \mathbf{b}_{\ell\mathrm{s}} = \mathbf{b}_{\mathrm{ss}}, \quad \text{at } A_{\ell\mathrm{s}} \tag{A.60}$$

$$0 = k_\mathrm{s}\nabla^2\mathbf{b}_{\mathrm{ss}} - \varepsilon_\mathrm{s}^{-1}(\mathbf{c}_{\mathrm{ss}}^{\mathrm{s}\ell} + \mathbf{c}_{\mathrm{ss}}^{\mathrm{sg}}), \quad \text{in the s-phase} \tag{A.61}$$

$$\text{Periodicity:} \quad \mathbf{b}_{\ell\mathrm{s}}(\mathbf{r}+l_i) = \mathbf{b}_{\ell\mathrm{s}}(\mathbf{r}), \quad \mathbf{b}_{\mathrm{gs}}(\mathbf{r}+l_i) = \mathbf{b}_{\mathrm{gs}}(\mathbf{r}), \quad \mathbf{b}_{\mathrm{ss}}(\mathbf{r}+l_i) = \mathbf{b}_{\mathrm{ss}}(\mathbf{r}), \quad i = 1,2,3 \tag{A.62}$$

$$\text{Average:} \quad \langle\mathbf{b}_{\ell\mathrm{s}}\rangle^{\ell} = 0, \quad \langle\mathbf{b}_{\mathrm{gs}}\rangle^{\mathrm{g}} = 0, \quad \langle\mathbf{b}_{\mathrm{ss}}\rangle^{\mathrm{s}} = 0 \tag{A.63}$$

We have adopted the following notations

$$\mathbf{c}_{\mathrm{gs}}^{\mathrm{g}\ell} = \frac{k_{\mathrm{g}}}{V}\int_{A_{\mathrm{g}\ell}} \mathbf{n}_{\mathrm{g}\ell}\cdot\nabla\mathbf{b}_{\mathrm{gs}}\,\mathrm{d}A,$$

$$\mathbf{c}_{\mathrm{gs}}^{\mathrm{gs}} = \frac{k_{\mathrm{g}}}{V}\int_{A_{\mathrm{gs}}} \mathbf{n}_{\mathrm{gs}}\cdot\nabla\mathbf{b}_{\mathrm{gs}}\,\mathrm{d}A = -\mathbf{c}_{\mathrm{ss}}^{\mathrm{sg}} - \frac{k_{\mathrm{s}}}{V}\int_{A_{\mathrm{sg}}} \mathbf{n}_{\mathrm{sg}}\,\mathrm{d}A \tag{A.64}$$

$$\mathbf{c}_{\ell\mathrm{s}}^{\ell\mathrm{g}} = \frac{k_{\ell}}{V}\int_{A_{\ell\mathrm{g}}} \mathbf{n}_{\ell\mathrm{g}}\cdot\nabla\mathbf{b}_{\ell\mathrm{s}}\,\mathrm{d}A,$$

$$\mathbf{c}_{\ell\mathrm{s}}^{\ell\mathrm{s}} = \frac{k_{\ell}}{V}\int_{A_{\ell\mathrm{s}}} \mathbf{n}_{\ell\mathrm{s}}\cdot\nabla\mathbf{b}_{\ell\mathrm{s}}\,\mathrm{d}A = -\mathbf{c}_{\mathrm{ss}}^{\mathrm{s}\ell} - \frac{k_{\mathrm{s}}}{V}\int_{A_{\mathrm{s}\ell}} \mathbf{n}_{\mathrm{s}\ell}\,\mathrm{d}A \tag{A.65}$$

$$\mathbf{c}_{\mathrm{ss}}^{\mathrm{s}\ell} = \frac{k_{\mathrm{s}}}{V}\int_{A_{\mathrm{s}\ell}} \mathbf{n}_{\mathrm{s}\ell}\cdot\nabla\mathbf{b}_{\mathrm{ss}}\,\mathrm{d}A, \quad \mathbf{c}_{\mathrm{ss}}^{\mathrm{sg}} = \frac{k_{\mathrm{s}}}{V}\int_{A_{\mathrm{sg}}} \mathbf{n}_{\mathrm{sg}}\cdot\nabla\mathbf{b}_{\mathrm{ss}}\,\mathrm{d}A \tag{A.66}$$

Appendix B. Definitions of the effective transport coefficients

Thermal dispersion tensors

$\langle T_{\mathrm{g}}\rangle^{\mathrm{g}}$-equation:

$$\mathbf{K}_{\mathrm{gg}} = \varepsilon_{\mathrm{g}}k_{\mathrm{g}}\mathbf{I} + \frac{k_{\mathrm{g}}}{V}\int_{A_{\mathrm{gs}}} \mathbf{n}_{\mathrm{gs}}\mathbf{b}_{\mathrm{gg}}\,\mathrm{d}A - (\rho C_p)_{\mathrm{g}}\langle\widetilde{\mathbf{v}}_{\mathrm{g}}\mathbf{b}_{\mathrm{gg}}\rangle \tag{B.1}$$

$$\mathbf{K}_{\mathrm{g}\ell} = \frac{k_{\mathrm{g}}}{V}\int_{A_{\mathrm{gs}}} \mathbf{n}_{\mathrm{gs}}\mathbf{b}_{\mathrm{g}\ell}\,\mathrm{d}A - (\rho C_p)_{\mathrm{g}}\langle\widetilde{\mathbf{v}}_{\mathrm{g}}\mathbf{b}_{\mathrm{g}\ell}\rangle \tag{B.2}$$

$$\mathbf{K}_{\mathrm{gs}} = \frac{k_{\mathrm{g}}}{V}\int_{A_{\mathrm{gs}}} \mathbf{n}_{\mathrm{gs}}\mathbf{b}_{\mathrm{gs}}\,\mathrm{d}A - (\rho C_p)_{\mathrm{g}}\langle\widetilde{\mathbf{v}}_{\mathrm{g}}\mathbf{b}_{\mathrm{gs}}\rangle \tag{B.3}$$

$\langle T_{\ell}\rangle^{\ell}$-equation:

$$\mathbf{K}_{\ell\mathrm{g}} = \frac{k_{\ell}}{V}\int_{A_{\ell\mathrm{s}}} \mathbf{n}_{\ell\mathrm{s}}\mathbf{b}_{\ell\mathrm{g}}\,\mathrm{d}A - (\rho C_p)_{\ell}\langle\widetilde{\mathbf{v}}_{\ell}\mathbf{b}_{\ell\mathrm{g}}\rangle \tag{B.4}$$

$$\mathbf{K}_{\ell\ell} = \varepsilon_{\ell}k_{\ell}\mathbf{I} + \frac{k_{\ell}}{V}\int_{A_{\ell\mathrm{s}}} \mathbf{n}_{\ell\mathrm{s}}\mathbf{b}_{\ell\ell}\,\mathrm{d}A - (\rho C_p)_{\ell}\langle\widetilde{\mathbf{v}}_{\ell}\mathbf{b}_{\ell\ell}\rangle \tag{B.5}$$

$$\mathbf{K}_{\ell\mathrm{s}} = \frac{k_{\ell}}{V}\int_{A_{\ell\mathrm{s}}} \mathbf{n}_{\ell\mathrm{s}}\mathbf{b}_{\ell\mathrm{s}}\,\mathrm{d}A - (\rho C_p)_{\ell}\langle\widetilde{\mathbf{v}}_{\ell}\mathbf{b}_{\ell\mathrm{s}}\rangle \tag{B.6}$$

$\langle T_{\mathrm{s}}\rangle^{\mathrm{s}}$-equation:

$$\mathbf{K}_{\mathrm{sg}} = \frac{k_{\mathrm{s}}}{V}\int_{A_{\mathrm{s}\ell}} \mathbf{n}_{\mathrm{s}\ell}\mathbf{b}_{\mathrm{sg}}\,\mathrm{d}A + \frac{k_{\mathrm{s}}}{V}\int_{A_{\mathrm{sg}}} \mathbf{n}_{\mathrm{sg}}\mathbf{b}_{\mathrm{sg}}\,\mathrm{d}A \tag{B.7}$$

$$\mathbf{K}_{\mathrm{s}\ell} = \frac{k_{\mathrm{s}}}{V}\int_{A_{\mathrm{s}\ell}} \mathbf{n}_{\mathrm{s}\ell}\mathbf{b}_{\mathrm{s}\ell}\,\mathrm{d}A + \frac{k_{\mathrm{s}}}{V}\int_{A_{\mathrm{sg}}} \mathbf{n}_{\mathrm{sg}}\mathbf{b}_{\mathrm{s}\ell}\,\mathrm{d}A \tag{B.8}$$

$$\mathbf{K}_{\mathrm{ss}} = \varepsilon_{\mathrm{s}}k_{\mathrm{s}}\mathbf{I} + \frac{k_{\mathrm{s}}}{V}\int_{A_{\mathrm{s}\ell}} \mathbf{n}_{\mathrm{s}\ell}\mathbf{b}_{\mathrm{ss}}\,\mathrm{d}A + \frac{k_{\mathrm{s}}}{V}\int_{A_{\mathrm{sg}}} \mathbf{n}_{\mathrm{sg}}\mathbf{b}_{\mathrm{ss}}\,\mathrm{d}A \tag{B.9}$$

Velocity like coefficients

$\langle T_{\mathrm{g}}\rangle^{\mathrm{g}}$-equation:

$$\mathbf{u}_{\mathrm{gg}} = \mathbf{c}_{\mathrm{gg}}^{\mathrm{g}\ell} + \mathbf{c}_{\mathrm{gg}}^{\mathrm{gs}} \tag{B.10}$$

$$\mathbf{u}_{\mathrm{g}\ell} = \mathbf{c}_{\mathrm{g}\ell}^{\mathrm{g}\ell} + \mathbf{c}_{\mathrm{g}\ell}^{\mathrm{gs}} \tag{B.11}$$

$$\mathbf{u}_{\mathrm{gs}} = \mathbf{c}_{\mathrm{gs}}^{\mathrm{g}\ell} + \mathbf{c}_{\mathrm{gs}}^{\mathrm{gs}} \tag{B.12}$$

$$\mathbf{d}_{\ell\mathrm{i}}^{\mathrm{g}} = (\rho C_p)_{\mathrm{g}}\langle\widetilde{\mathbf{v}}_{\mathrm{g}}s_{\ell\mathrm{i}}^{\mathrm{g}}\rangle - \frac{k_{\mathrm{g}}}{V}\int_{A_{\mathrm{gs}}} \mathbf{n}_{\mathrm{gs}}s_{\ell\mathrm{i}}^{\mathrm{g}}\,\mathrm{d}A \tag{B.13}$$

$$\mathbf{d}_{\mathrm{gi}}^{\mathrm{g}} = (\rho C_p)_{\mathrm{g}}\langle\widetilde{\mathbf{v}}_{\mathrm{g}}s_{\mathrm{gi}}^{\mathrm{g}}\rangle - \frac{k_{\mathrm{g}}}{V}\int_{A_{\mathrm{g}\ell}} \mathbf{n}_{\mathrm{g}\ell}\,\mathrm{d}A - \frac{k_{\mathrm{g}}}{V}\int_{A_{\mathrm{gs}}} \mathbf{n}_{\mathrm{gs}}s_{\mathrm{gi}}^{\mathrm{g}}\,\mathrm{d}A \tag{B.14}$$

$$\mathbf{d}_{\mathrm{si}}^{\mathrm{g}} = (\rho C_p)_{\mathrm{g}}\langle\widetilde{\mathbf{v}}_{\mathrm{g}}s_{\mathrm{si}}^{\mathrm{g}}\rangle - \frac{k_{\mathrm{g}}}{V}\int_{A_{\mathrm{gs}}} \mathbf{n}_{\mathrm{gs}}s_{\mathrm{si}}^{\mathrm{g}}\,\mathrm{d}A \tag{B.15}$$

$\langle T_{\ell}\rangle^{\ell}$-equation:

$$\mathbf{u}_{\ell\mathrm{g}} = \mathbf{c}_{\ell\mathrm{g}}^{\ell\mathrm{g}} + \mathbf{c}_{\ell\mathrm{g}}^{\ell\mathrm{s}} \tag{B.16}$$

$$\mathbf{u}_{\ell\ell} = \mathbf{c}_{\ell\ell}^{\ell\mathrm{g}} + \mathbf{c}_{\ell\ell}^{\ell\mathrm{s}} \tag{B.17}$$

$$\mathbf{u}_{\ell\mathrm{s}} = \mathbf{c}_{\ell\mathrm{s}}^{\ell\mathrm{g}} + \mathbf{c}_{\ell\mathrm{s}}^{\ell\mathrm{s}} \tag{B.18}$$

$$\mathbf{d}_{\ell\mathrm{i}}^{\ell} = (\rho C_p)_{\ell}\langle\widetilde{\mathbf{v}}_{\ell}s_{\ell\mathrm{i}}^{\ell}\rangle - \frac{k_{\ell}}{V}\int_{A_{\ell\mathrm{g}}} \mathbf{n}_{\ell\mathrm{g}}\,\mathrm{d}A - \frac{k_{\ell}}{V}\int_{A_{\ell\mathrm{s}}} \mathbf{n}_{\ell\mathrm{s}}s_{\ell\mathrm{i}}^{\ell}\,\mathrm{d}A \tag{B.19}$$

$$\mathbf{d}_{\mathrm{gi}}^{\ell} = (\rho C_p)_{\ell}\langle\widetilde{\mathbf{v}}_{\ell}s_{\mathrm{gi}}^{\ell}\rangle - \frac{k_{\ell}}{V}\int_{A_{\ell\mathrm{s}}} \mathbf{n}_{\ell\mathrm{s}}s_{\mathrm{gi}}^{\ell}\,\mathrm{d}A \tag{B.20}$$

$$\mathbf{d}_{\mathrm{si}}^{\ell} = (\rho C_p)_{\ell}\langle\widetilde{\mathbf{v}}_{\ell}s_{\mathrm{si}}^{\ell}\rangle - \frac{k_{\ell}}{V}\int_{A_{\ell\mathrm{s}}} \mathbf{n}_{\ell\mathrm{s}}s_{\mathrm{si}}^{\ell}\,\mathrm{d}A \tag{B.21}$$

$\langle T_{\mathrm{s}}\rangle^{\mathrm{s}}$-equation:

$$\mathbf{u}_{\mathrm{sg}} = \mathbf{c}_{\mathrm{sg}}^{\mathrm{s}\ell} + \mathbf{c}_{\mathrm{sg}}^{\mathrm{sg}} \tag{B.22}$$

$$\mathbf{u}_{\mathrm{s}\ell} = \mathbf{c}_{\mathrm{s}\ell}^{\mathrm{s}\ell} + \mathbf{c}_{\mathrm{s}\ell}^{\mathrm{sg}} \tag{B.23}$$

$$\mathbf{u}_{\mathrm{ss}} = \mathbf{c}_{\mathrm{ss}}^{\mathrm{s}\ell} + \mathbf{c}_{\mathrm{ss}}^{\mathrm{sg}} \tag{B.24}$$

$$\mathbf{d}_{\ell\mathrm{i}}^{\mathrm{s}} = -\frac{k_{\mathrm{s}}}{V}\int_{A_{\mathrm{s}\ell}} \mathbf{n}_{\mathrm{s}\ell}s_{\ell\mathrm{i}}^{\mathrm{s}}\,\mathrm{d}A - \frac{k_{\mathrm{s}}}{V}\int_{A_{\mathrm{sg}}} \mathbf{n}_{\mathrm{sg}}s_{\ell\mathrm{i}}^{\mathrm{s}}\,\mathrm{d}A \tag{B.25}$$

$$\mathbf{d}_{\mathrm{gi}}^{\mathrm{s}} = -\frac{k_{\mathrm{s}}}{V}\int_{A_{\mathrm{s}\ell}} \mathbf{n}_{\mathrm{s}\ell}s_{\mathrm{gi}}^{\mathrm{s}}\,\mathrm{d}A - \frac{k_{\mathrm{s}}}{V}\int_{A_{\mathrm{sg}}} \mathbf{n}_{\mathrm{sg}}s_{\mathrm{gi}}^{\mathrm{s}}\,\mathrm{d}A \tag{B.26}$$

$$\mathbf{d}_{\mathrm{si}}^{\mathrm{s}} = -\frac{k_{\mathrm{s}}}{V}\int_{A_{\mathrm{s}\ell}} \mathbf{n}_{\mathrm{s}\ell}s_{\mathrm{si}}^{\mathrm{s}}\,\mathrm{d}A - \frac{k_{\mathrm{s}}}{V}\int_{A_{\mathrm{sg}}} \mathbf{n}_{\mathrm{sg}}s_{\mathrm{si}}^{\mathrm{s}}\,\mathrm{d}A \tag{B.27}$$

Appendix C. Results for one-dimensional unit cells

The six closure problems previously listed that provide the effective properties of the three-equation model can be solved numerically according to previous development for two-equation models, see for instance Quintard et al. [53]. Following Chella et al. [20], a direct numerical simulation of the two-phase flow at the pore-scale can be used to provide the required velocity field and the inter-

face position. Analytical solutions of closure problems are also available in the case of simple unit cells. In this section, some analytical results for effective properties are presented for stratified systems and Chang's unit cells. Obviously, these unit cells cannot capture all the feature of a real system, for instance the effect of the velocity field and the complex topology of both liquid–vapor interface and solid boundary. However, these simple unit cells are instructive and allow to illustrate the behavior of the effective transport coefficients.

C.1. Stratified unit cell

The six closure problems were solved analytically for the stratified unit cell represented in Fig. 10 following the methodology outlined in [52]. Phases repartition of such a unit cell are the s–ℓ–g configuration and the s–g–ℓ configuration. The first refers to liquid being the wetting phase while the latter refers to liquid being the non-wetting phase. The characteristic length of the unit cell H is defined according to the thickness of the strata ℓ_ℓ, ℓ_g and ℓ_s by $H = \ell_\ell + \ell_g + \ell_s$. The volume fractions of the three phases are given by $\ell_\ell = \varepsilon_\ell H$, $\ell_g = \varepsilon_g H$ and $\ell_s = \varepsilon_s H$.

In this paper, we focus on the s–g–ℓ configuration, corresponding results for the other configuration can be obtained easily with subscript permutation. The flow is assumed to be laminar and it corresponds to a co-current liquid–vapor flow along the x-axis. The velocity profiles corresponding to the s–g–ℓ configuration can be expressed as

$$u_g = \frac{\langle u_g\rangle^g}{\varepsilon_g(3\varepsilon_\ell + 2\varepsilon_g)}\left(3(\varepsilon_g+\varepsilon_\ell)^2 - 12\left(\frac{y}{H}\right)^2\right) \tag{C.1}$$

$$u_\ell = \frac{3\langle u_\ell\rangle^\ell}{2\varepsilon_\ell^2 + 3\varepsilon_g\eta_{\ell g}(\varepsilon_g + 2\varepsilon_\ell)}\left(\varepsilon_\ell^2 + \varepsilon_g\eta_{\ell g}(2\varepsilon_\ell+\varepsilon_g) - 4\left(\frac{y}{H}\right)^2\right) \tag{C.2}$$

where $\eta_{\ell g} = \eta_\ell/\eta_g$ denotes the viscosity ratio. These velocity profiles are plotted in Fig. 11 for $\eta_{\ell g} > 1$. Solutions of the closure problems IV, V, VI for the mapping vectors leads to the following dimensionless form of the non-traditional convective coefficients

$$\frac{H(\mathbf{d}^\ell_{\ell i})_x}{k_g} = -\frac{2}{5}\frac{\varepsilon_\ell^2 k_\ell}{(2\varepsilon_\ell^2 + 3\varepsilon_g\eta_{\ell g}(2\varepsilon_\ell+\varepsilon_g))k_g}\varepsilon_\ell Pe_\ell \tag{C.3}$$

$$\frac{H(\mathbf{d}^g_{gi})_x}{k_g} = \frac{1}{10}\frac{2\varepsilon_s\kappa_{gs}(7\varepsilon_g + 15\varepsilon_\ell) - 3\varepsilon_g^2}{(2\varepsilon_g+3\varepsilon_\ell)(3\varepsilon_g + 4\varepsilon_s\kappa_{gs})}\varepsilon_g Pe_g \tag{C.4}$$

$$\frac{H(\mathbf{d}^g_{si})_x}{k_g} = \frac{1}{10}\frac{3\varepsilon_g(5\varepsilon_\ell + 3\varepsilon_g)}{(2\varepsilon_g+3\varepsilon_\ell)(3\varepsilon_g + 4\varepsilon_s\kappa_{gs})}\varepsilon_g Pe_g \tag{C.5}$$

and for this particular geometry we found analytically that

$$(\mathbf{u}_{\ell\ell})_x = (\mathbf{d}^\ell_{\ell i})_x, \quad (\mathbf{u}_{gg})_x = (\mathbf{d}^g_{gi})_x, \quad (\mathbf{u}_{sg})_x = (\mathbf{d}^g_{si})_x \tag{C.6}$$

The transport coefficients which are not listed are equal to zero. In these equations, κ_{gs} represents the conductivity ratio k_g/k_s and the cell Péclet number Pe_β is defined as

$$Pe_\beta = (\rho C_p)_\beta \frac{\langle u_\beta\rangle^\beta H}{k_\beta}, \quad \beta = g, \ell \tag{C.7}$$

We recall that Stokes equations have been used in the calculation of the velocity fields, thus the Péclet number is the only relevant dimensionless parameter rather than independent Reynolds and Prandtl numbers as was outlined in [57]. One can also determine the dominant

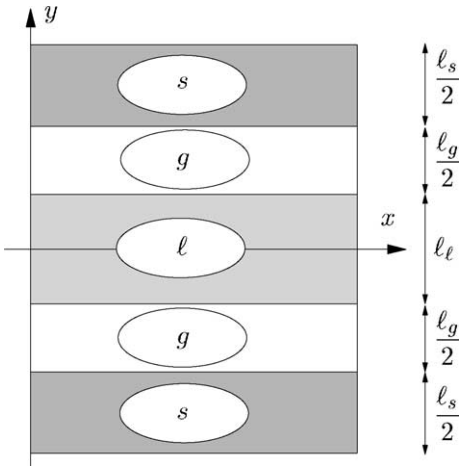

Fig. 10. Stratified unit cell—s–g–ℓ configuration.

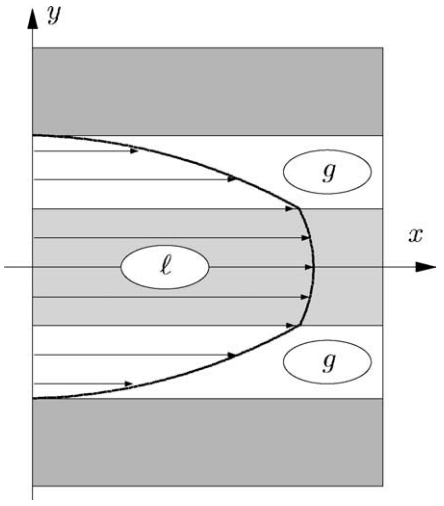

Fig. 11. Velocity profiles for the s–g–ℓ configuration.

thermal dispersion tensor from Eq. (B.1) and the coupling thermal dispersion tensors from Eqs. (B.2) and (B.3), the results are given below

$$\frac{(\mathbf{K}_{gg})_{xx}}{k_g} = \varepsilon_g\left(1 + \frac{3}{2800}\frac{\varepsilon_g(9\varepsilon_g^2 + 35\varepsilon_\ell(1-\varepsilon_s))}{(2\varepsilon_g + 3\varepsilon_\ell)^2(3\varepsilon_g + 4\varepsilon_s\kappa_{gs})}\varepsilon_g^2 Pe_g^2 + \frac{1}{2800}\frac{\varepsilon_s\kappa_{gs}(99\varepsilon_g^2 + \varepsilon_\ell(350\varepsilon_g + 315\varepsilon_\ell))}{(2\varepsilon_g + 3\varepsilon_\ell)^2(3\varepsilon_g + 4\varepsilon_s\kappa_{gs})}\varepsilon_g^2 Pe_g^2\right) \tag{C.8}$$

$$\frac{(\mathbf{K}_{gg})_{yy}}{k_g} = \frac{\varepsilon_g^2}{\varepsilon_g + \varepsilon_s\kappa_{gs}} \tag{C.9}$$

$$\frac{(\mathbf{K}_{\ell\ell})_{xx}}{k_g} = \frac{\varepsilon_\ell k_\ell}{k_g}\left(1 + \frac{1}{175}\frac{\varepsilon_\ell^4}{(2\varepsilon_\ell^2 + 3\varepsilon_g\eta_{\ell g}(2\varepsilon_\ell + \varepsilon_g))^2}\varepsilon_\ell^2 Pe_\ell^2\right) \tag{C.10}$$

$$\frac{(\mathbf{K}_{\ell\ell})_{yy}}{k_g} = \frac{\varepsilon_\ell k_\ell}{k_g} \tag{C.11}$$

$$\frac{(\mathbf{K}_{gs})_{yy}}{k_g} = \frac{(\mathbf{K}_{sg})_{yy}}{k_g} = \frac{\varepsilon_g\varepsilon_s}{\varepsilon_g + \varepsilon_s\kappa_{gs}} \tag{C.12}$$

$$\frac{(\mathbf{K}_{ss})_{xx}}{k_g} = \frac{\varepsilon_s}{\kappa_{gs}} \tag{C.13}$$

$$\frac{(\mathbf{K}_{ss})_{yy}}{k_g} = \frac{\varepsilon_s^2}{\varepsilon_g + \varepsilon_s\kappa_{gs}} \tag{C.14}$$

Finally, we give below the dimensionless form of the heat exchange coefficients that appears in the macroscopic equations (54)–(56)

$$\frac{H^2 h_{\ell i}^{\ell g}}{k_g} = \frac{12k_\ell}{\varepsilon_\ell k_g} \tag{C.15}$$

$$\frac{H^2 h_{gi}^{g\ell}}{k_g} = \frac{24(3\varepsilon_g + 2\varepsilon_s\kappa_{gs})}{\varepsilon_g(3\varepsilon_g + 4\varepsilon_s\kappa_{gs})} \tag{C.16}$$

$$\frac{H^2 h_{gi}^{gs}}{k_g} = \frac{72}{3\varepsilon_g + 4\varepsilon_s\kappa_{gs}} \tag{C.17}$$

$$\frac{H^2 h_{si}^{gs}}{k_g} = \frac{-48}{3\varepsilon_g + 4\varepsilon_s\kappa_{gs}} \tag{C.18}$$

$$\frac{H^2 h_{si}^{g\ell}}{k_g} = \frac{-24}{3\varepsilon_g + 4\varepsilon_s\kappa_{gs}} \tag{C.19}$$

Here again the transport coefficients which are not listed are equal to zero.

C.2. Chang's unit cell

Analytical results have also been obtained for the three-phase version of the Chang's unit cell [19] shown in Fig. 12. The radii r_1 and r_2 corresponding to the s–g–ℓ configuration are defined by $r_1 = R\sqrt{\varepsilon_s}$ and $r_2 = R\sqrt{\varepsilon_s + \varepsilon_g}$, where R is the characteristic length of the unit cell. Details concerning the methodology of resolution of the closure problems can be found in Quintard and Whitaker [58]. Here, we give only the results concerning the dimensionless form of the heat transfer coefficients corresponding to the s–g–ℓ configuration:

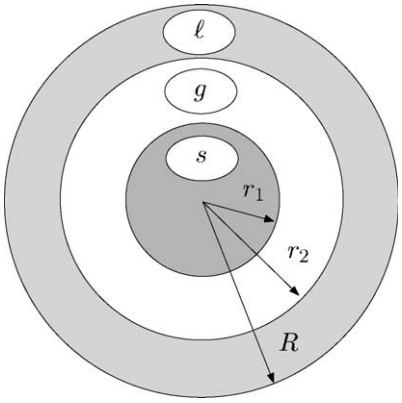

Fig. 12. Chang's unit cell.

$$\frac{h_{\ell i}^{\ell g} R^2}{k_g} = \frac{-8\varepsilon_\ell^2 k_\ell}{k_g(\varepsilon_\ell(\varepsilon_\ell + 2) + 4\ln\sqrt{1-\varepsilon_\ell})} \tag{C.20}$$

$$\frac{h_{gi}^{g\ell} R^2}{k_g} = \frac{8\varepsilon_g(\varepsilon_g(\kappa_{gs} - 2) + 4(1-\varepsilon_\ell)\xi)}{\varepsilon_g((\varepsilon_g - 2\varepsilon_s)\kappa_{gs} - 4\varepsilon_g) + 4(\varepsilon_s^2(\kappa_{gs} - 1) + (1-\varepsilon_\ell)^2)\xi} \tag{C.21}$$

$$\frac{h_{gi}^{gs} R^2}{k_g} = \frac{16\varepsilon_g(\varepsilon_g - 2\varepsilon_s\xi)}{\varepsilon_g((\varepsilon_g - 2\varepsilon_s)\kappa_{gs} - 4\varepsilon_g) + 4(\varepsilon_s^2(\kappa_{gs} - 1) + (1-\varepsilon_\ell)^2)\xi} \tag{C.22}$$

$$\frac{h_{si}^{gs} R^2}{k_g} = \frac{-8\varepsilon_g(\varepsilon_g - 2\varepsilon_s) - 32\varepsilon_s^2\xi}{\varepsilon_g((\varepsilon_g - 2\varepsilon_s)\kappa_{gs} - 4\varepsilon_g) + 4(\varepsilon_s^2(\kappa_{gs} - 1) + (1-\varepsilon_\ell)^2)\xi} \tag{C.23}$$

$$\frac{h_{si}^{g\ell} R^2}{k_g} = \frac{-8\varepsilon_g(\varepsilon_g + 2\varepsilon_s) + 32\varepsilon_s(1-\varepsilon_\ell)\xi}{\varepsilon_g((\varepsilon_g - 2\varepsilon_s)\kappa_{gs} - 4\varepsilon_g) + 4(\varepsilon_s^2(\kappa_{gs} - 1) + (1-\varepsilon_\ell)^2)\xi} \tag{C.24}$$

Here the parameter ξ is defined as

$$\xi = \ln\sqrt{\frac{1-\varepsilon_\ell}{\varepsilon_s}}$$

Despite the simplicity of the Chang's unit cell, the expressions for the heat exchange coefficients are more complicated than those corresponding to the stratified medium and they correspond to a more relevant physical description. Indeed, when evaporation or condensation occurs, the liquid volume fraction changes and the Chang's unit cell takes into account the change in the

liquid–vapor exchange area per unit volume while the stratified unit cell considers constant exchange area per unit volume for all the values of the liquid volume fraction.

References

[1] A. Ahmadi, A. Aigueperse, M. Quintard, Calculation of the effective properties describing active dispersion in porous media: from simple to complex unit cells, Adv. Water Resour. 24 (2001) 423–438.

[2] W.H. Amarasooriya, T.G. Theofanous, Premixing of steam explosions: a three-fluid model, Nucl. Eng. Des. 126 (1991) 23–39.

[3] S. Angelini, W.W. Yuen, T.G. Theofanous, Premixing-related behavior of steam explosions, Nucl. Eng. Des. 155 (1995) 115–157.

[4] T. Arbogast, Analysis of the simulation of single phase flow through a naturally fractured reservoir, SIAM J. Numer. Anal. 26 (1) (1989) 12–29.

[5] T. Arbogast, J. Douglas, U. Hornung, Derivation of the double porosity model of single phase flow via homogenization theory, SIAM J. Numer. Anal. 21 (1990) 823–836.

[6] K. Atkhen, G. Berthoud, Experimental and numerical investigations on debris bed coolability in a 3D homogeneous configuration, in: Proceedings of ICONE 9, Ninth International Conference on Nuclear Engineering, Nice Acropolis, France, 8–12 April 2001.

[7] J.L. Auriault, Nonsaturated deformable porous media: quasistatics, Transport Porous Media 2 (1987) 45–64.

[8] J.L. Auriault, P. Royer, Double conductivity media: a comparison between phenomenological and homogenization approaches, Int. J. Heat Mass Transfer 36 (10) (1993) 2613–2621.

[9] K.H. Bang, Numerical prediction of forced convection film boiling heat transfer from a sphere, Int. J. Heat Mass Transfer 37 (16) (1994) 2415–2424.

[10] G.D. Barenblatt, I.P. Zheltov, I.N. Kochina, Basic concepts in the theory of homogeneous liquids in fissured rocks, J. Appl. Math. (USSR) 24 (5) (1960) 1286–1303.

[11] C. Béchaud, F. Duval, F. Fichot, M. Quintard, M. Parent, Debris bed coolability using a 3-D two phase model in a porous medium, in: Proceedings of ICONE 9, Ninth International Conference on Nuclear Engineering, Nice Acropolis, France, April 2001.

[12] B. Berkowitz, H. Scher, On characterization of anomalous dispersion in porous media and fractured media, Water Resour. Res. 31 (1995) 1461–1466.

[13] G. Berthoud, M. Valette, Development of a multidimensional model for the premixing phase of a fuel–coolant interaction, Nucl. Eng. Des. 149 (1994) 409–418.

[14] H. Bertin, M. Panfilov, M. Quintard, Two types of transient phenomena and full relaxation macroscale model for single phase flow through double porosity media, Transport Porous Media 39 (1) (2000) 73–96.

[15] J.F. Bloch, J.L. Auriault, Heat transfer in nonsaturated porous media: modelling by homogenisation, Transport Porous Media 30 (1998) 301–321.

[16] A. Bouddour, J.L. Auriault, M. Mhamdi-Alaoui, J.F. Bloch, Heat and mass transfer in wet porous media in presence of evaporation–condensation, Int. J. Heat Mass Transfer 41 (1998) 2263–2277.

[17] P. Bousquet-Mélou, A. Neculae, B. Goyeau, M. Quintard, Averaged solute transport during solidification of a binary mixture: active dispersion in dendritic structures, Metall. Mater. Trans. B 33B (3) (2002) 365–376.

[18] R.G. Carbonell, S. Whitaker, Heat and mass transfer in porous media, in: J. Bear, M.Y. Corapcioglu (Eds.), Fundamentals of Transport Phenomena in Porous Media, Martinus Nijhoff Publishers, Dordrecht, 1984, pp. 123–198.

[19] H.C. Chang, Effective diffusion and conduction in two-phase media: a unified approach, AIChE J. 29 (5) (1983) 846–853.

[20] R. Chella, D. Lasseux, M. Quintard, Multiphase, multicomponent fluid flow in homogeneous and heterogeneous porous media, Revue de l'Institut Français du Pétrole 53 (3) (1998) 335–346.

[21] Z.-X. Chen, Transient flow of slightly compressible fluids through double-porosity, double-permeability systems - a state-of-the-art review, Transport Porous Media 4 (1989) 147–184.

[22] M. Chung, I. Catton, Post-dryout heat transfer in a multidimensional porous bed, Nucl. Eng. Des. 128 (1991) 289–304.

[23] J.H. Cushman, T.R. Ginn, Nonlocal dispersion in media with continuously evolving scales of heterogeneity, Transport Porous Media 13 (1993) 123–138.

[24] J.V. Daurelle, F. Topin, R. Occelli, Modeling of coupled heat and mass transfers with phase change in a porous medium: application to superheated steam drying, Numer. Heat Transfer A (33) (1988) 39–63.

[25] E. Décossin, Numerical investigations on particulate debris bed coolability: critical analysis of the Silfide experimental project, in: Ninth International Topical Meeting on Nuclear Reactor Thermal Hydraulics (NURETH-9), October 1999, San Francisco, CA.

[26] A. de Swann, Analytic solutions for determining naturally fractured reservoir properties by well testing, SPE J. (1976) 117–122.

[27] F. Duval, Modélisation du renoyage d'un lit de particules: contribution à l'estimation des propriétés de transport macroscopiques. Mécanique energétique, Institut National Polytechnique, Toulouse, November 2002.

[28] P.W. Egolf, H. Manz, Theory and modeling of phase change materials with and without mushy regions, Int. J. Heat Mass Transfer 37 (8) (1994) 2917–2924.

[29] H.I. Ene, D. Polisevski, Thermal Flow in Porous Media, D. Reidel Publishing Company, Dordrecht, 1987.

[30] F. Fichot, F. Duval, N. Trégourés, C. Béchaud, M. Quintard, The impact of thermal non-equilibrium and large-scale 2D/3D effects on debris bed reflooding and coolability, Nucl. Eng. Des., in press.

[31] J. Florio, J.B. Henderson, F.L. Test, R. Hariharan, A study of the effects of the assumption of local-thermal equilibrium on the overall thermally-induced response of a decomposing, glass-filled polymer composite, Int. J. Heat Mass Transfer 34 (1) (1991) 135–147.

[32] G. Grangeot, M. Quintard, S. Whitaker, Heat transfer in packed beds: interpretation of experiments in terms of one- and two-equation models, in: 10th International Heat Transfer Conference, Brighton, vol. 5, 1994, pp. 291–296.
[33] W.G. Gray, A derivation of the equations for multi-phase transport, Chem. Eng. Sci. 30 (1975) 229–233.
[34] K. Grosser, R.G. Carbonell, A. Cavero, A.E. Sáez, Lateral thermal dispersion in gas–liquid cocurrent downflow through packed beds, AIChE J. 42 (10) (1996) 2977–2983, R & D Notes.
[35] J. Hager, S. Whitaker, Vapor–liquid jump conditions within a porous medium: results for mass and energy, Transport Porous Media 40 (2000) 73–111.
[36] J. Hager, S. Whitaker, The thermodynamic significance of the local volume averaged temperature, Transport Porous Media 46 (2002) 19–35.
[37] J. Hager, R. Wimmerstedt, S. Whitaker, Steam drying a bed of porous spheres: theory and experiment, Chem. Eng. Sci. 55 (2000) 1675–1698.
[38] M. Kaviany, Principles of Heat Transfer in Porous Media, in: Mechanical Engineering Series, second ed., Springer, Berlin, 1995.
[39] D.L. Koch, J.F. Brady, Anomalous diffusion in heterogeneous porous media, Phys. Fluids 5 (1988) 965–973.
[40] P. Landereau, B. Noetinger, M. Quintard, Quasi-steady two-equation models for diffusive transport in fractured porous media: large-scale properties for densely fractured systems, Adv. Water Resour. 24 (2001) 863–876.
[41] D. Lasseux, M. Quintard, S. Whitaker, Determination of permeability tensors for two-phase flow in homogeneous porous media: theory, Transport Porous Media 24 (1996) 107–137.
[42] J. Levec, R.G. Carbonell, Longitudinal and lateral thermal dispersion in packed beds. Part I. Theory, AIChE J. 31 (4) (1985) 581–590.
[43] J. Levec, R.G. Carbonell, Longitudinal and lateral thermal dispersion in packed beds. Part II. Comparison between theory and experiment, AIChE J. 31 (4) (1985) 591–602.
[44] V.V. Likhanskii, A.I. Loboiko, O.V. Khoruzhii, Two-phase convection in a porous medium with nonuniform volume heat release, Atomic Energy 82 (3) (1997) 180–186.
[45] R.J. Lipinski, A coolability model for post-accident nuclear reactor debris, Nucl. Technol. 65 (1984) 53–66.
[46] S.G. Liter, M. Kaviany, Pool-boiling CHF enhancement by modulated porous-layer coating: theory and experiment, Int. J. Heat Mass Transfer 44 (2001) 4287–4311.
[47] C. Moyne, Two-equation model for a diffusive process in porous media using the volume averaging method with an unsteady-state closure, Adv. Water Resour. 20 (2–3) (1997) 63–76.
[48] C. Moyne, S. Didierjean, A. Souto, O.T. da Silveira, Thermal dispersion in porous media: one-equation model, Int. J. Heat Mass Transfer 43 (2000) 3853–3867.
[49] Y.S. Ng, S. Banerjee, Two-phase flow characteristics during controlled oscillation reflooding of a hot vertical tube, Technical Report NP-2821, EPRI, 1983.
[50] A.A.M. Oliveira, M. Kaviany, Nonequilibrium in the transport of heat and reactants in combustion in porous media, Progr. Energy Combust. Sci. 27 (2001) 523–545.
[51] I.K. Park, G.C. Park, K.H. Bang, Multiphase flow modeling of molten material–vapor–liquid mixtures in thermal nonequilibrium, KSME Int. J. 14 (5) (2000) 553–561.
[52] F. Petit, F. Fichot, M. Quintard, Ecoulement diphasique en milieux poreux: modéle à non-équilibre local, Int. J. Thermal Sci. 38 (1999) 239–249.
[53] M. Quintard, M. Kaviany, S. Whitaker, Two-medium treatment of heat transfer in porous media: numerical results for effective properties, Adv. Water Resour. 20 (1997) 77–94.
[54] M. Quintard, B. Ladevie, S. Whitaker, Effect of homogeneous and heterogeneous source terms on the macroscopic description of heat transfer in porous media, in: Symposium on Energy Engineering in the 21st Century, vol. 2, Hong Kong, January 2000, pp. 482–489.
[55] M. Quintard, S. Whitaker, One- and two-equation models for transient diffusion processes in two-phase systems, in: Advances in Heat Transfer, vol. 23, Academic Press, New York, 1993, pp. 369–464.
[56] M. Quintard, S. Whitaker, Transport in ordered and disordered porous media: volume-averaged equations, closure problems, and comparison with experiment, Chem. Eng. Sci. 48 (14) (1993) 2537–2564.
[57] M. Quintard, S. Whitaker, Convection, dispersion, and interfacial transport of contaminants: homogeneous porous media, Adv. Water Resour. 17 (1994) 221–239.
[58] M. Quintard, S. Whitaker, Local thermal equilibrium for transient heat conduction: theory and comparison with numerical experiments, Int. J. Heat Mass Transfer 38 (15) (1995) 2779–2796.
[59] M. Quintard, S. Whitaker, Transport in chemically and mechanically heterogeneous porous media. I. Theoretical development of region-averaged equations for slightly compressible single-phase flow, Adv. Water Resour. 19 (1) (1996) 29–47.
[60] M. Quintard, S. Whitaker, Dissolution of an immobile phase during flow in porous media, Indust. Eng. Chem. Res. 38 (3) (1999) 833–844.
[61] M. Quintard, S. Whitaker, Theoretical analysis of transport in porous media, in: H. Hadim, K. Vafai, M. Decker (Eds.), Handbook of Heat Transfer in Porous Media, Inc. New York, 2000, pp. 1–52 (chapter 1).
[62] T. Schulenberg, U. Müller, An improved model for two-phase flow through beds of coarse particles, Int. J. Multiphase Flow 13 (1) (1987) 87–97.
[63] M. Sözen, K. Vafai, Analysis of the non-thermal equilibrium condensing flow of a gas through a packed bed, Int. J. Heat Mass Transfer 33 (6) (1990) 1247–1261.
[64] K. Vafai, M. Sozen, Analysis of energy and momentum transport for fluid flow through a porous bed, J. Heat Transfer 112 (1990) 690–699.
[65] C.Y. Wang, C. Beckermann, A two-phase mixture model of liquid-gas flow and heat transfer in capillary porous media. I. Formulation, Int. J. Heat Mass Transfer 36 (11) (1993) 2747–2758.
[66] S. Whitaker, A simple geometrical derivation of the spatial averaging theorem, Chem. Eng. Education 19 (1985) 18–21, 50–52.
[67] S. Whitaker, Flow in porous media. II. The governing equations for immiscible, two-phase flow, Transport Porous Media 1 (1986) 105–125.

[68] S. Whitaker, Improved constraints for the principle of local thermal equilibrium, Ind. Eng. Chem. Res. 30 (1991) 983–997.
[69] S. Whitaker, Coupled transport in multiphase systems: a theory of drying, in: Advances in Heat Transfer, vol. 31, Academic Press, New-York, 1998, pp. 1–102.
[70] S. Whitaker, The Method of Volume Averaging, in: Theory and Applications of Transport in Porous Media, vol. 13, Kluwer Academic Publishers, Dordrecht, 1999.
[71] A.W. Woods, Liquid and vapor flow in superheated rock, Ann. Rev. Fluid Mech. 31 (1999) 171–199.
[72] G. Yadigaroglu, R.A. Nelson, V. Teschendorff, Y. Murao, J. Kelly, D. Bestion, Modeling of reflooding, Nucl. Eng. Des. 145 (1993) 1–35.
[73] F. Zanotti, R.G. Carbonell, Development of transport equations for multiphase systems. I. General development for two phase systems, Chem. Eng. Sci. 39 (2) (1984) 263–278.
[74] H.Y. Zhang, X.Y. Huang, A two-equation analysis of convection heat transfer in porous media, Transport Porous Media 44 (2001) 305–324.